

AD-A245 109



u

2

NAVAL POSTGRADUATE SCHOOL Monterey, California



DTIC
SELECTE
JAN 27, 1992
S B D

THESIS

FAST REACTION MISSILE CONTROL
FOR POINT DEFENSE

by

Hakan Karazeybek

December, 1991

Thesis Advisor:

Harold A. Titus

92-01953

Approved for public release; distribution is unlimited.

92 1 23 063

Unclassified

Security Classification of this page

REPORT DOCUMENTATION PAGE

1a Report Security Classification Unclassified				1b Restrictive Markings			
2a Security Classification Authority				3 Distribution Availability of Report Approved for public release; distribution is unlimited.			
2b Declassification/Downgrading Schedule				5 Monitoring Organization Report Number(s)			
4 Performing Organization Report Number(s)				7a Name of Monitoring Organization Naval Postgraduate School			
6a Name of Performing Organization Naval Postgraduate School		6b Office Symbol (If Applicable) 32		7b Address (city, state, and ZIP code) Monterey, CA 93943-5000			
6c Address (city, state, and ZIP code) Monterey, CA 93943-5000				9 Procurement Instrument Identification Number			
8a Name of Funding/Sponsoring Organization		8b Office Symbol (If Applicable)		10 Source of Funding Numbers			
8c Address (city, state, and ZIP code)				Program Element Number	Project No	Task No	Work Unit Accession No
11 Title (Include Security Classification) FAST REACTION MISSILE CONTROL FOR POINT DEFENSE							
12 Personal Author(s) Hakan Karazeybek							
13a Type of Report Master's Thesis		13b Time Covered From To		14 Date of Report (year, month, day) December 1991		15 Page Count 76	
16 Supplementary Notation The views expressed in this thesis are those of the author and do not reflect the official policy or position of the Department of Defense or the U.S. Government.							
17 Cosati Codes			18 Subject Terms (continue on reverse if necessary and identify by block number)				
Field	Group	Subgroup	Minimum Time Control, Bang-Bang Control, Missile, Miss Distance, Line-of-Sight				
19 Abstract (continue on reverse if necessary and identify by block number) Optimal Control Theory is revisited. A minimum time control rule for a third order regulator is found. A third order missile model is developed. Minimum time control is applied to the fast reaction missile defense problem. The results are compared with Proportional Navigation. The states controlled in the minimum time application are the derivatives of Line-of-Sight angle and the vertical distance and derivatives between missile and the target.							
20 Distribution/Availability of Abstract <input checked="" type="checkbox"/> unclassified/unlimited <input type="checkbox"/> same as report <input type="checkbox"/> DTIC users				21 Abstract Security Classification Unclassified			
22a Name of Responsible Individual Harold A. Titus				22b Telephone (Include Area code) (408) 646-2560		22c Office Symbol EC/Ts	

DD FORM 1473, 84 MAR

83 APR edition may be used until exhausted

security classification of this page

All other editions are obsolete

Unclassified

Approved for public release; distribution is unlimited.

Fast Reaction Missile Control
for Point Defense

by

Hakan Karazeybek
Lieutenant J.G., Turkish Navy
B.S., Turkish Naval Academy

Submitted in partial fulfillment
of the requirements for the degree of

MASTER OF SCIENCE IN ELECTRICAL ENGINEERING

from the

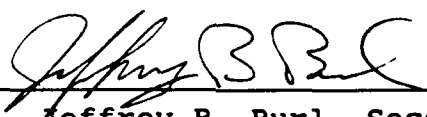
NAVAL POSTGRADUATE SCHOOL
December 1991

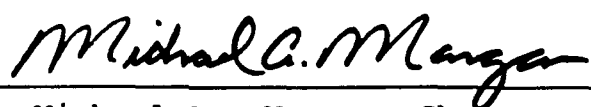
Author:


Hakan Karazeybek

Approved by:


Harold A. Titus, Thesis Advisor


Jeffrey B. Burl, Second Reader


Michael A. Morgan, Chairman
Department of Electrical and Computer Engineering

ABSTRACT

Optimal Control Theory is revisited. A minimum time control rule for a third order regulator is found. A third order missile model is developed. Minimum time control is applied to the fast reaction missile defense problem. The results are compared with Proportional Navigation. The states controlled in the minimum time application are the derivatives of Line-of-Sight angle and the vertical distance and derivatives between missile and the target.



Accession For	
NTIS GRA&I	<input checked="" type="checkbox"/>
DTIC TAB	<input type="checkbox"/>
Unannounced	<input type="checkbox"/>
Justification	
By _____	
Distribution/ _____	
Availability Codes	
Dist	Avail and/or Special
A-1	

TABLE OF CONTENTS

I. INTRODUCTION	1
II. MINIMUM TIME CONTROL	3
A. OPTIMUM CONTROL	3
B. TIME OPTIMAL CONTROL	3
1. Problem Definition	3
2. Problem Solution	4
C. TIME OPTIMAL CONTROL EXAMPLE	7
1. Uncoupled System	8
2. Problem Solution	10
3. Simulation of The Third Order System . .	16
III. MISSILE GUIDANCE AND CONTROL	20
A. INTRODUCTION	20
B. GUIDANCE	20
C. TYPES OF GUIDANCE LAW	22
1. Pursuit Guidance	22
2. Line-Of-Sight Guidance	23
3. Proportional Navigation Guidance	23
D. CONTROL SYSTEM	23
IV. MISSILE MODEL AND SIMULATION	27
A. ASSUMPTIONS	27
B. TWO DIMENSIONAL MISSILE TARGET GEOMETRY . . .	27
C. MISSILE MODEL	30

1.	System Signal Flow Graph	30
2.	Guidance System	30
3.	Flight Control System	32
4.	Missile Dynamics	32
D.	PROPORTIONAL NAVIGATION SIMULATION	33
1.	Speed Advantage of Missile	35
2.	Speed Advantage of Target	39
V.	MISSILE APPLICATION OF THIRD ORDER CONTROLLER	43
A.	MISSILE AND THIRD ORDER REGULATOR	43
B.	GUIDANCE BY VERTICAL DISTANCE BETWEEN MISSILE AND TARGET	45
C.	GUIDANCE BY DERIVATIVES OF σ	51
VI.	CONCLUSIONS	56
	APPENDIX	57
1.	PROPNAV.M	57
2.	YYDYDD.M	60
3.	SIGMDER.M	63
4.	SWTH_LAW.M	67
	REFERENCES	68
	INITIAL DISTRIBUTION LIST	69

ACKNOWLEDGEMENTS

I would like to thank my advisor, Hal Titus for his guidance and constructive criticism which made this study a great learning experience. I would also like to express my gratitude for my friends who supported me emotionally throughout this time. Finally, many thanks go to 57 million Turkish citizens who provided my education here in Naval Postgraduate School.

I. INTRODUCTION

The expectation of any missile system is to hit the target with high probability; in other words, to make the terminal miss distance between the missile and target as small as possible. For thousands of years projectile weapons have had a lack of control after launching. This is detrimental to hit probability. Guided missiles have overcome this situation by being controlled after launching.

Currently, there are three guidance laws for tactical missiles. These laws are Pursuit Guidance, Line-of-Sight Guidance and Proportional Guidance. A missile can employ one or more of these guidance laws. Guidance at the terminal phase of the missile flight is most important.

A point defense system may be required to hit an attacking missile that has a speed advantage. Instead of following an expensive method such as designing new systems against these targets, current systems may be upgraded.

Present work applies a different control to a surface-to-air missile. In Chapter II, a minimum time control problem is defined and solved for a third order regulator. In Chapter III, the three different missile guidance laws are described. Acceleration effects on missile velocity is also explained. In

Chapter IV, a missile model is formed and the missile/target engagement scenario is simulated by using Proportional Navigation Guidance. In Chapter V, the third order minimum time solution is applied to the missile/target engagement simulation.

II. MINIMUM TIME CONTROL

A. OPTIMUM CONTROL

Control system design is a trial and error process utilizing various techniques to reach a desired outcome. Classically, the performance of a system is defined in terms of time and frequency, i.e., rise time, overshoot, gain and phase margins. However, complex multiple-input, multiple-output systems require a more elaborate design than the classical design. For example, when controlling the attitude of a satellite to minimize fuel consumption, optimal control theory is required to design a satisfactory system, incorporating the complications of multiple input and output variables. Optimal control theory can be defined as:

"The objective of optimal control theory is to determine the control signals that will cause a process to satisfy the physical constraints and at the same time minimize (or maximize) some performance criterion." [Ref. 1:p. 1]

B. TIME OPTIMAL CONTROL

1. Problem Definition

In minimum time problems, the objective is to drive a system from an arbitrary initial state to a desired state in minimum time. Mathematically, the problem is to transfer a system, that is,

$$\dot{x}(t) = Ax(t) + Bu(t) \quad (2.1)$$

or,

$$\dot{x}(t) = f(x(t), u(t), t) \quad (2.2)$$

from an arbitrary initial state to a desired state by minimizing

$$J = \int_{t_0}^{t_f} dt = t_f - t_0 \quad (2.3)$$

Control effort u is constrained by a maximum value, such as

$$|u| \leq N \quad (2.4)$$

The final state may be any point in the state-space. In this study, the final point is the origin of the state-space. When the final state is the origin, in a linear, stationary, n th order system as defined in Equation (1.1), the problem is referred to as the stationary, linear regulator, minimum-time problem.

2. Problem Solution

In this section, minimum time control for single input systems will be described. From Pontryagin[1], it is

known that the performance measurement J defined at Equation (2.3) can be minimized by minimizing the Hamiltonian which is in the form of

$$H = 1 + p^T A x + p^T B u \quad (2.5)$$

In this equation, u minimizes the Hamiltonian by operating at its maximum value with the opposite sign of its coefficient $p^T B$. Thus, u can be written as

$$u = -N * \text{sign}(p^T B) \quad (2.6)$$

An optimal time control can be solved for a system, if all the eigenvalues of A have non-positive parts. The control u is called the *bang-bang* control which occurs at its maximum values as either $+N$ or $-N$. The number of switches between these values is at most $n-1$ times for systems with real roots depending on the initial position of the system in state space where n is the order of the system.

For an existing control, there are two trajectories possible reaching to the origin; one for $u=+N$ and one for $u=-N$. These are zero trajectory curves that finally carry the system to the origin. These trajectories divide the state-space into two parts.

Some possible optimal trajectories for a second order system can be seen in Figure 2.1. The solid line curves are the zero trajectory curves. The state of the system above these curves follows a parabolic path parallel to the $-N$ zero trajectory curve, with the control effort of $-N$; the state below these curves has control effort $+N$ and follows a parabolic path parallel to the $+N$ zero trajectory. These curves are illustrated with dashed line curves. The control on these curves switches once. At points A and B the control switches from $+N$ to $-N$ and at points C and D from $-N$ to $+N$.

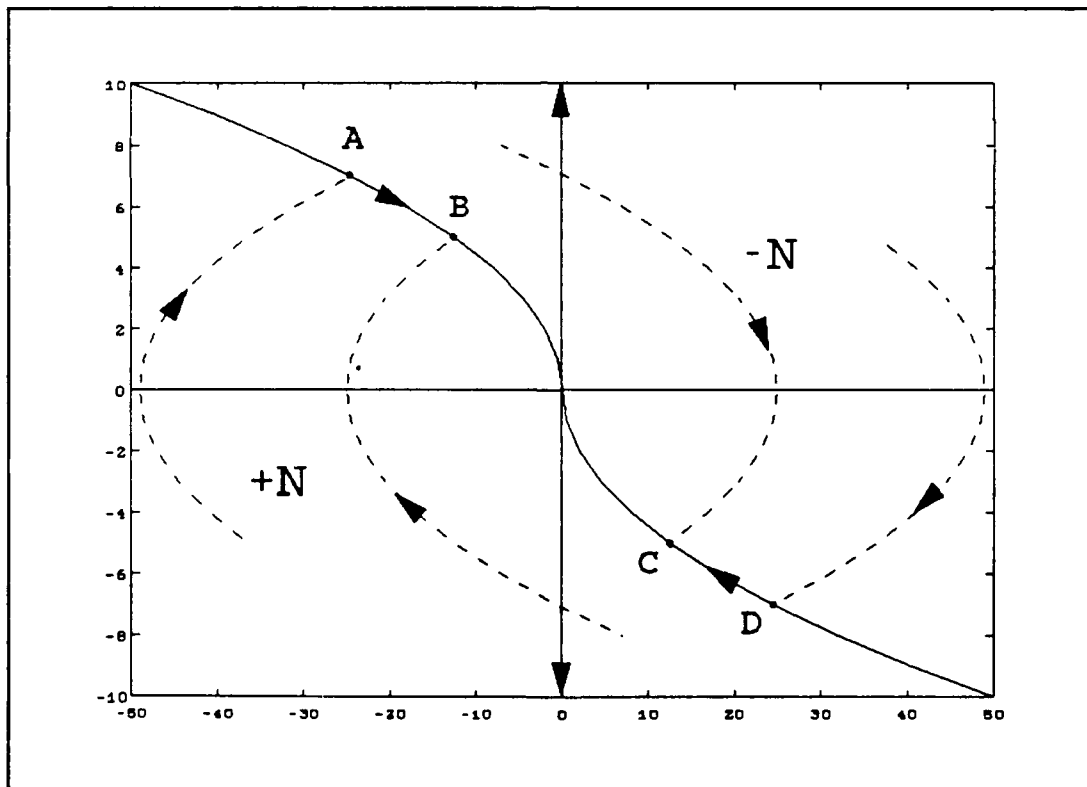


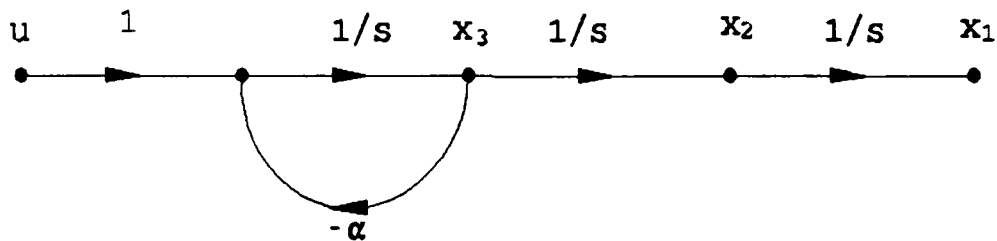
Figure 2.1 Minimum Time Trajectory Curves

If these trajectories are described geometrically in terms of state variables, the control function can be defined as the switching function. This control function decides the sign of the control and in which conditions the control will change its sign in state-space.

Since the final state is the origin, but the initial state is any place in state-space, it is better to solve the u in negative time with zero initial conditions. Zero initial conditions in negative time define the origin, end point of the positive time problem. In this method, all minimum time trajectories are defined in a generalized equation in terms of states. This process is explained in Reference 1.

C. TIME OPTIMAL CONTROL EXAMPLE

As an example, switching law can be found for the following third order system.



This system is similar to the missile model which will be described in the following chapters, so the switching law which will be solved in this section will be used for the minimum time application of the missile problem.

The state-space of the system is

$$\begin{bmatrix} \dot{x}_1 \\ \dot{x}_2 \\ \dot{x}_3 \end{bmatrix} = \begin{bmatrix} 0 & 1 & 0 \\ 0 & 0 & 1 \\ 0 & 0 & -\alpha \end{bmatrix} \begin{bmatrix} x_1 \\ x_2 \\ x_3 \end{bmatrix} + \begin{bmatrix} 0 \\ 0 \\ 1 \end{bmatrix} u \quad (2.7)$$

The transfer function of the system is

$$\frac{X(s)}{U(s)} = \frac{1}{s^2(s+\alpha)} \quad (2.8)$$

Eigenvalues are real and negative, so we can have a solution. Since the system is third order, there are at most two switches in the control depending on the initial position of the system in the state-space.

1. Uncoupled System

The switching law for the system defines hyper-surfaces in the state-space instead of curves in the state-plane for a second order system. Transformation of the system into an uncoupled system provides an easier definition for the switching law. This is accomplished by taking a partial fraction expansion of the transfer function and defining each

state with respect to control input and assigning a new state vector to each eigenvalue, which is

$$x = Gy \quad (2.9)$$

Uncoupled state-space is found by following

$$G\dot{y} = AGy + Bu$$

so,

$$\dot{y} = G^{-1}AGy + G^{-1}Bu \quad (2.10)$$

Description of each state with respect to control is

$$x_1(s) = \frac{u(s)}{s^2(s+\alpha)} = \frac{1/\alpha}{s^2} - \frac{1/\alpha^2}{s} + \frac{1/\alpha^2}{s+\alpha} \quad (2.11)$$

$$x_2(s) = \frac{1/\alpha}{s} - \frac{1/\alpha}{s+\alpha} \quad (2.12)$$

$$x_3(s) = \frac{1}{s+\alpha} \quad (2.13)$$

From these equations, G and G⁻¹ matrices are found as

$$G = \begin{bmatrix} \frac{1}{\alpha} & -\frac{1}{\alpha^2} & \frac{1}{\alpha^2} \\ 0 & \frac{1}{\alpha} & -\frac{1}{\alpha} \\ 0 & 0 & 1 \end{bmatrix} \quad \text{and} \quad G^{-1} = \begin{bmatrix} \alpha & 1 & 0 \\ 0 & \alpha & 1 \\ 0 & 0 & 1 \end{bmatrix} \quad (2.14)$$

The uncoupled state-space system is

$$\begin{bmatrix} y_1 \\ y_2 \\ y_3 \end{bmatrix} = \begin{bmatrix} 0 & 1 & 0 \\ 0 & 0 & 0 \\ 0 & 0 & -\alpha \end{bmatrix} \begin{bmatrix} y_1 \\ y_2 \\ y_3 \end{bmatrix} + \begin{bmatrix} 0 \\ 1 \\ 1 \end{bmatrix} u \quad (2.15)$$

2. Problem Solution

The discretization of the system is

$$\phi = \mathcal{L}^{-1}((sI-A)^{-1}) = \begin{bmatrix} 1 & t & 0 \\ 0 & 1 & 0 \\ 0 & 0 & e^{-\alpha t} \end{bmatrix} \quad (2.16)$$

$$\Delta = \int_0^t \phi B dt = \begin{bmatrix} \frac{1}{2} t^2 \\ t \\ \frac{1}{\alpha} (1 - e^{-\alpha t}) \end{bmatrix} \quad (2.17)$$

Using these discrete time matrices, the discrete state-space equation is

$$\begin{bmatrix} y_1(t) \\ y_2(t) \\ y_3(t) \end{bmatrix} = \begin{bmatrix} 1 & t & 0 \\ 0 & 1 & 0 \\ 0 & 0 & e^{-\alpha t} \end{bmatrix} \begin{bmatrix} y_1(0) \\ y_2(0) \\ y_3(0) \end{bmatrix} + \begin{bmatrix} \frac{1}{2} t^2 \\ t \\ \frac{1}{\alpha} (1 - e^{-\alpha t}) \end{bmatrix} u(0) \quad (2.18)$$

The positive time difference equations are

$$y_1(t) = y_1(0) + y_2(0)t + \frac{1}{2}u(0)t^2 \quad (2.19)$$

$$y_2(t) = y_2(0) + u(0)t \quad (2.20)$$

$$y_3(t) = y_3(0)e^{-\alpha t} + \frac{u(0)}{\alpha}(1-e^{-\alpha t}) \quad (2.21)$$

In negative time with zero initial conditions the difference equations become

$$y_1(t) = \frac{1}{2}u(0)t^2 \quad (2.22)$$

$$y_2(t) = -u(0)t \quad (2.23)$$

$$y_3(t) = \frac{u(0)}{\alpha}(1-e^{\alpha t}) \quad (2.24)$$

By applying $u=+N$ to the system, we have Table 1 for one second intervals. For $u=-N$, we have Table 2. Zero trajectory curves are defined by Tables 1 and 2.

As a next step, the curves before final switching are to be defined. This can be accomplished by equating positive time equations to the negative time zero trajectory curve equations.

TABLE 1
ZERO TRAJECTORY SET (u=+N)

u=+N	t=1	t=2	t=3
$y_1(t)$	$\frac{1}{2}N$	$2N$	$\frac{9}{2}N$
$y_2(t)$	$-N$	$-2N$	$-3N$
$y_3(t)$	$\frac{N}{\alpha}(1-e^\alpha)$	$\frac{N}{\alpha}(1-e^{2\alpha})$	$\frac{N}{\alpha}(1-e^{3\alpha})$

TABLE 2
ZERO TRAJECTORY SET (u=-N)

u=-N	t=1	t=2	t=3
$y_1(t)$	$-\frac{1}{2}N$	$2N$	$-\frac{9}{2}N$
$y_2(t)$	N	$2N$	$3N$
$y_3(t)$	$-\frac{N}{\alpha}(1-e^\alpha)$	$-\frac{N}{\alpha}(1-e^{2\alpha})$	$-\frac{N}{\alpha}(1-e^{3\alpha})$

At the time control switches from $u=-N$ to $u=+N$, negative time equations with control effort $u=+N$ are equal to positive time equations with control effort $u=-N$. These sets of equations are

$$y_1(t) = \frac{1}{2}N = y_1(0) + y_2(0) - \frac{1}{2}Nt^2 \quad (2.25)$$

$$y_2(t) = -N = y_2(0) - Nt \quad (2.26)$$

$$y_3(t) = \frac{N}{\alpha}(1-e^{-\alpha t}) = y_3(0)e^{-\alpha t} - \frac{N}{\alpha}(1-e^{-\alpha t}) \quad (2.27)$$

At time t the control switches from $-N$ to $+N$. From Equation (2.26) we can get

$$t = 1 + \frac{y_2(0)}{N} \quad (2.28)$$

By putting t in Equations (2.27) and (2.28) we have

$$N = y_1(0) + \frac{y_2^2(0)}{2N} \quad (2.29)$$

$$0 = e^{-\alpha} e^{-\alpha \frac{y_2(0)}{N}} \left(y_3(0) + \frac{N}{\alpha} \right) - \frac{2N}{\alpha} + \frac{N}{\alpha} e^{\alpha} \quad (2.30)$$

By following the same steps, we can solve the set of equations for the control switches from $+N$ to $-N$ and obtain the family of curves shown in Table 3. A common solution from the Table 3 gives the switching law for the uncoupled system.

TABLE 3
SOLUTION SET FOR THE UNCOUPLED SYSTEM

$u=+N$	$t=1$	$N = y_1(0) + \frac{y_2^2(0)}{2N}$
		$0 = e^{-\alpha} e^{-\frac{\alpha y_2(0)}{N}} \left(y_2(0) + \frac{N}{\alpha} \right) - \frac{2N}{\alpha} + \frac{N}{\alpha} e^{\alpha}$
	$t=2$	$4N = y_1(0) + \frac{y_2^2(0)}{2N}$
		$0 = e^{-2\alpha} e^{-\frac{2\alpha y_2(0)}{N}} \left(y_2(0) + \frac{N}{\alpha} \right) - \frac{2N}{\alpha} + \frac{N}{\alpha} e^{2\alpha}$
	$t=3$	$9N = y_1(0) + \frac{y_2^2(0)}{2N}$
		$0 = e^{-3\alpha} e^{-\frac{3\alpha y_2(0)}{N}} \left(y_2(0) + \frac{N}{\alpha} \right) - \frac{2N}{\alpha} + \frac{N}{\alpha} e^{3\alpha}$
$u=-N$	$t=1$	$-N = y_1(0) - \frac{y_2^2(0)}{2N}$
		$0 = e^{-\alpha} e^{\frac{\alpha y_2(0)}{N}} \left(y_2(0) - \frac{N}{\alpha} \right) + \frac{2N}{\alpha} - \frac{N}{\alpha} e^{\alpha}$
	$t=2$	$-4N = y_1(0) - \frac{y_2^2(0)}{2N}$
		$0 = e^{-2\alpha} e^{\frac{2\alpha y_2(0)}{N}} \left(y_2(0) - \frac{N}{\alpha} \right) + \frac{2N}{\alpha} - \frac{N}{\alpha} e^{2\alpha}$
	$t=3$	$-9N = y_1(0) - \frac{y_2^2(0)}{2N}$
		$0 = e^{-3\alpha} e^{\frac{3\alpha y_2(0)}{N}} \left(y_2(0) - \frac{N}{\alpha} \right) + \frac{2N}{\alpha} - \frac{N}{\alpha} e^{3\alpha}$

From Table 3, it is defined ;

$$w = \text{sign}\left(y_1(0) + \frac{y_2(0)|y_2(0)|}{2N}\right) \quad (2.31)$$

$$f = y_1(0) + w \frac{y_2(0)}{2N} \quad (2.32)$$

$$z = \sqrt{\left|\frac{f}{N}\right|} \quad (2.33)$$

These common equations define the family of curves which is

$$0 = \left(e^{-z\alpha} e^{-w \frac{\alpha y_2(0)}{N}}\right) \left(y_3(0) + \frac{wN}{\alpha}\right) + w \left(-\frac{2N}{\alpha} + \frac{e^{z\alpha} N}{\alpha}\right) \quad (2.34)$$

Equations (2.31-34) give the switching law. The switching function for the uncoupled system is

$$u = -N \text{sign}\left(e^{-z\alpha - \frac{w\alpha y_2(0)}{N}} \left(y_3(0) + \frac{wN}{\alpha}\right) + w \left(-\frac{2N}{\alpha} + \frac{e^{z\alpha} N}{\alpha}\right)\right) \quad (2.35)$$

This switching equation is for the uncoupled system. For the normal state system we need to define the uncoupled states in terms of normal states. This can be done by the following equation

$$y = G^{-1}x \quad (2.36)$$

So the uncoupled states are expressed as

$$\begin{aligned} y_1 &= \alpha x_1 + x_2 \\ y_2 &= \alpha x_2 + x_3 \\ y_3 &= x_3 \end{aligned} \quad (2.37)$$

From Equations (2.36) and (2.37), the switching law in terms of normal states can be written as

$$u = -N \cdot \text{sign} \left(e^{-z\alpha} \frac{w(\alpha x_2(0) + x_3(0))}{N} \left(x_3(0) + \frac{wN}{\alpha} \right) + w \left(\frac{-2N}{\alpha} + \frac{e^{z\alpha} N}{\alpha} \right) \right) \quad (2.38)$$

Where z, w, f are also in terms of normal states.

3. Simulation of The Third Order System

The third order regulator is simulated with the switching law found in the previous section. It is seen that the control changes its sign at two times and drives the states of the system to the origin. The initial values for the simulation run are $x_1(0) = -0.5$, $x_2(0) = -0.5$, $x_3(0) = 0.5$. Figures 2.3-5 show that the states reach to zero. The control effort is in Figure 2.6. After the states reach to the origin, the control starts chattering or limit cycles. Since the simulation is in discrete time, the control moves back and forth between plus and minus zero trajectories around the origin. This movement causes the limit cycles. The sampling rate or time delay in control effort decides the magnitude of the limit cycle. Figures 2.6 and 2.7 show the second order parabolic relation between states x_1, x_2 and x_2, x_3 . System states follows a parabolic path in the second order state-plane.

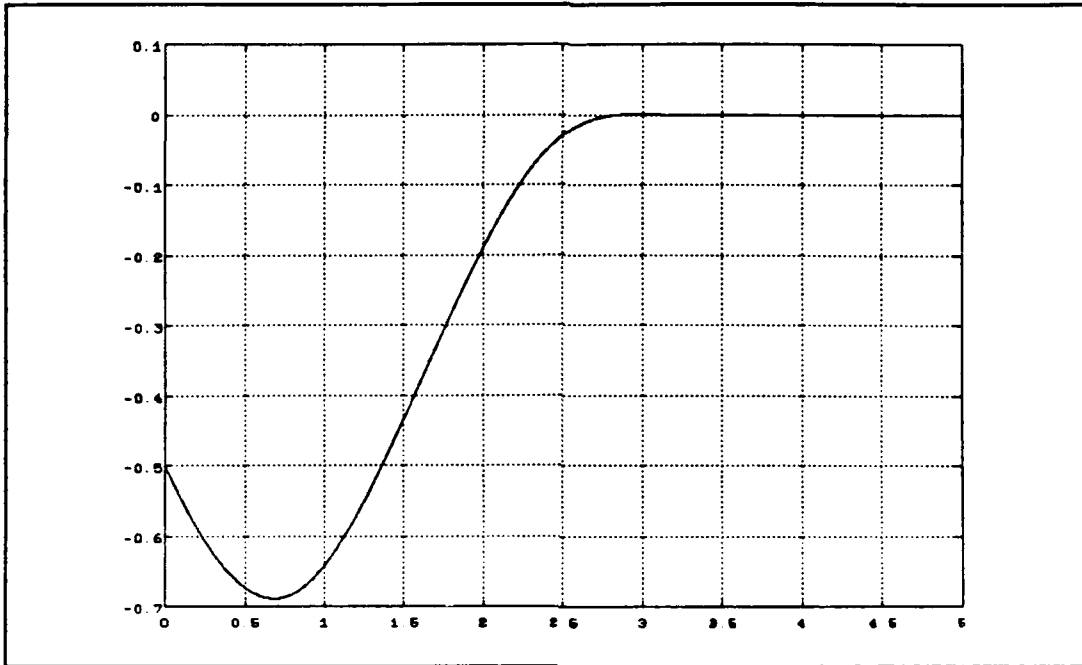


Figure 2.2 First State

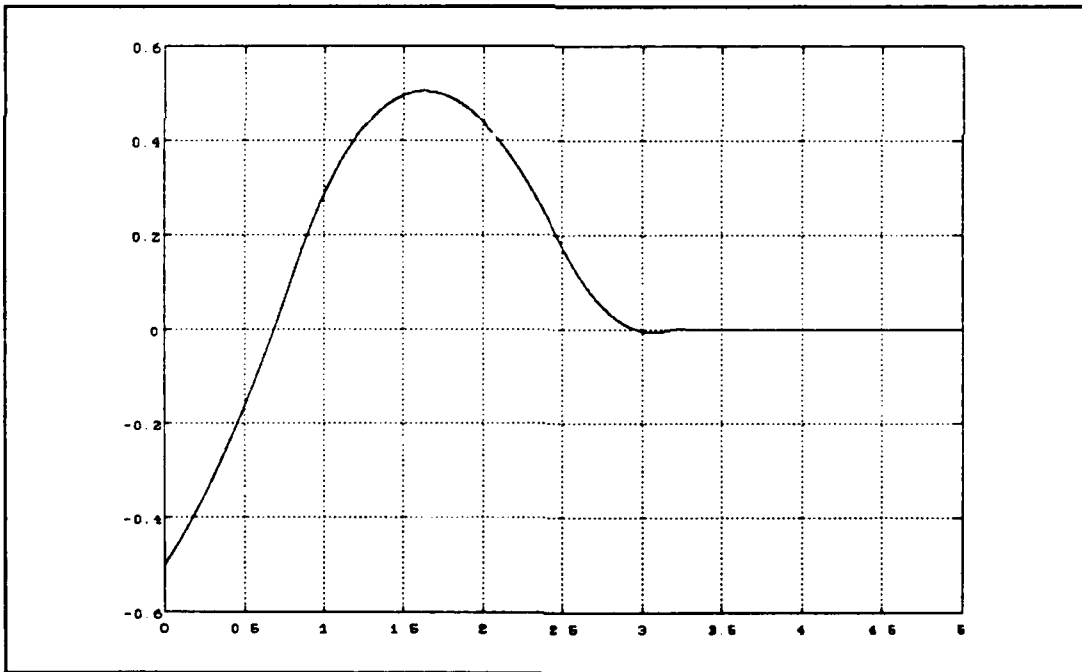


Figure 2.3 Second State

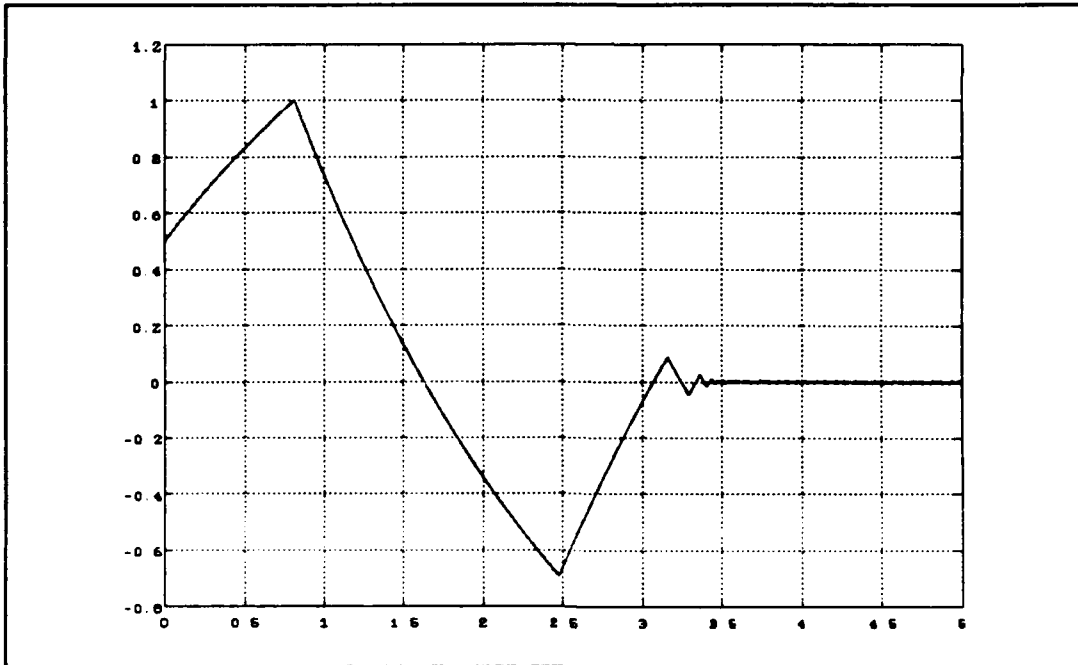


Figure 2.4 Third State

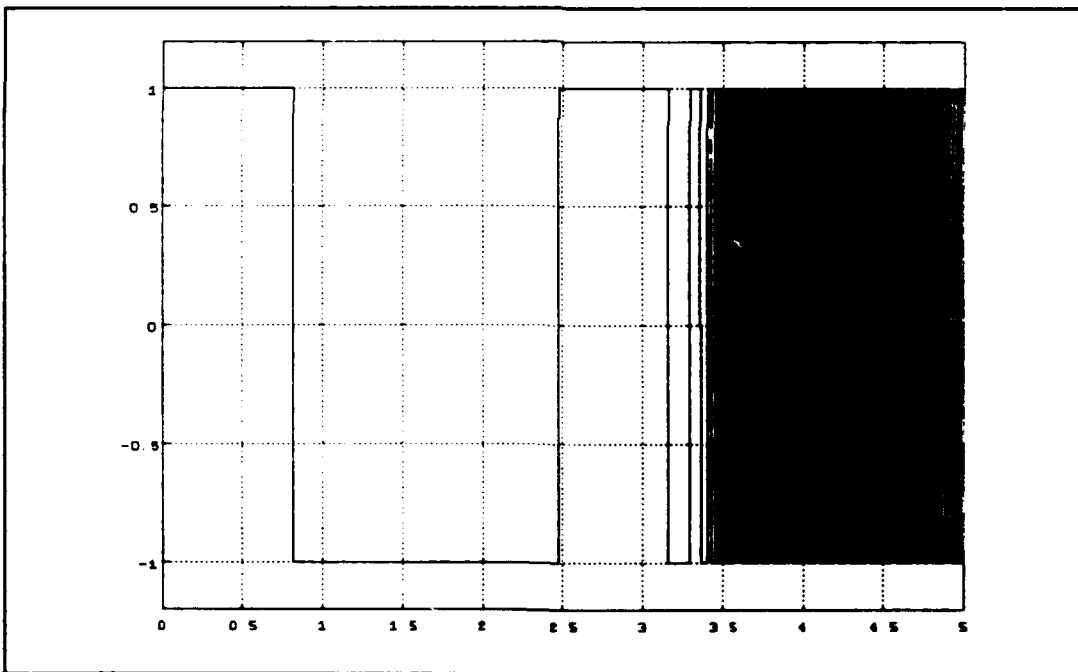


Figure 2.5 Control Effort

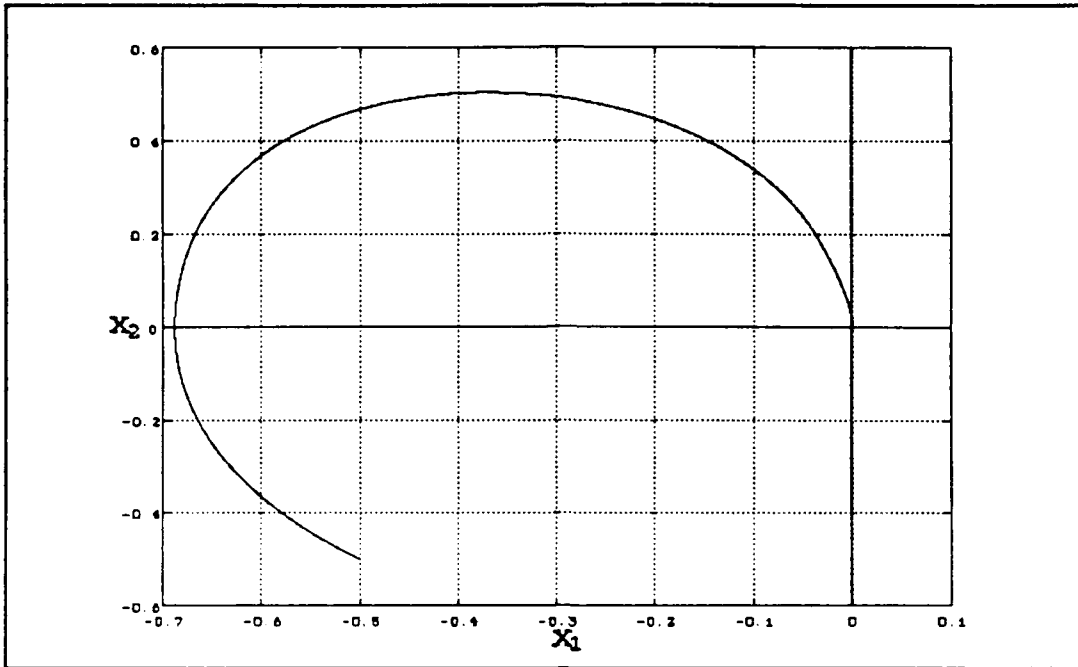


Figure 2.6 State-Plane for x_1 and x_2

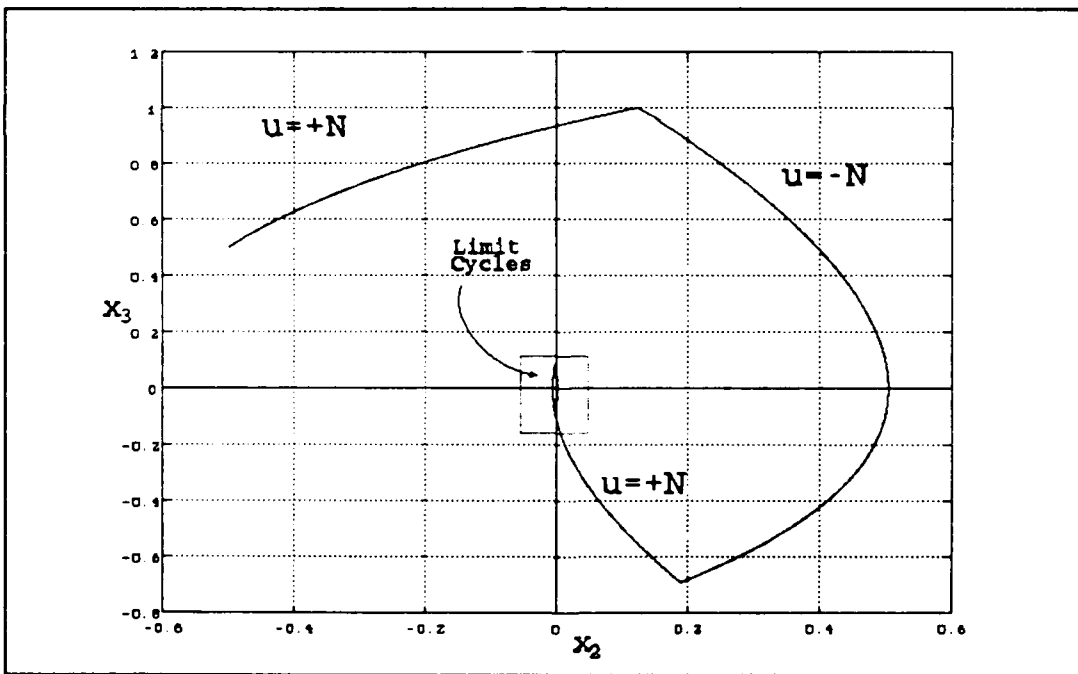


Figure 2.7 State-Plane for x_2 and x_3

III. MISSILE GUIDANCE AND CONTROL

A. INTRODUCTION

Guided missiles have much importance over other weapons because of their high probability of hitting their target. This high probability is the result of adjustments in missile movements to keep the missile on an intercept course despite target movements. The missile acts under commands from the guidance and control system. These systems keep the missile on an intercept course with the target. The guidance system applies the command to the missile body.

B. GUIDANCE

An unguided weapon may have an excessive miss distance because of the following reasons:

- Incorrect direction of launching;
- Perturbation of weapon by weather or wind;
- Unpredictable movement of the target after launching.

A good method to reduce miss distance and thus improve hit probability, is to use a closed loop system. A general form of a closed loop system is shown in Figure 3.1 [Ref 2. p. 71]. All guidance systems are particular examples of the general system in Figure 3.1.

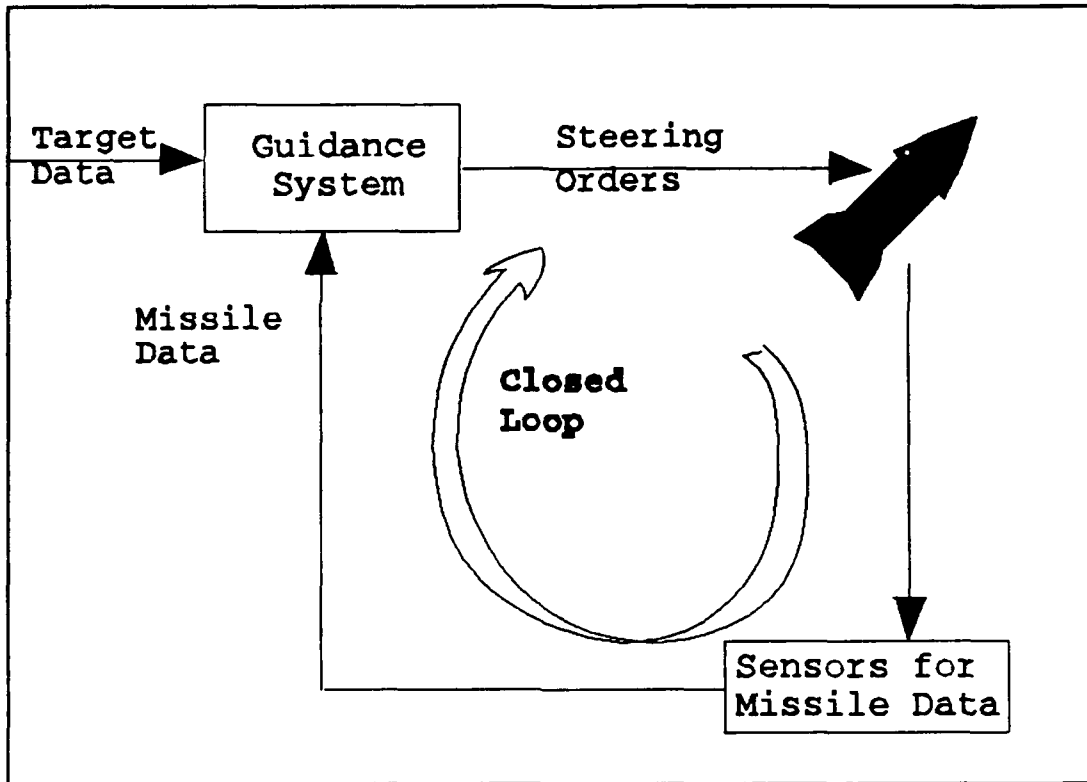


Figure 3.1 Closed Loop

Missile position and behavior is measured by an observation instrumentation which may be actually combined in the missile itself or may be situated on a remote platform such as a ship or an aircraft. This missile data is fed into the guidance computer with target data. The computer determines the maneuvers of the missile to improve its chances of hitting the target. Steering instructions, such as desired lateral acceleration in the pitch and yaw plane, are passed by the computer to the control system. The control system moves the control surfaces or determines the propulsive thrust. The resulting motion of the missile is measured by observation

instrumentation. The cycle continues with new observation data.

C. TYPES OF GUIDANCE LAW

1. Pursuit Guidance

Pursuit guidance is established by having the missile velocity vector directed toward the target. The missile always stays along the line-of-sight from missile to the target. This guidance is effective against slow moving or oncoming targets which have slow line-of-sight rates. The pursuit guidance is illustrated in Figure 3.2.

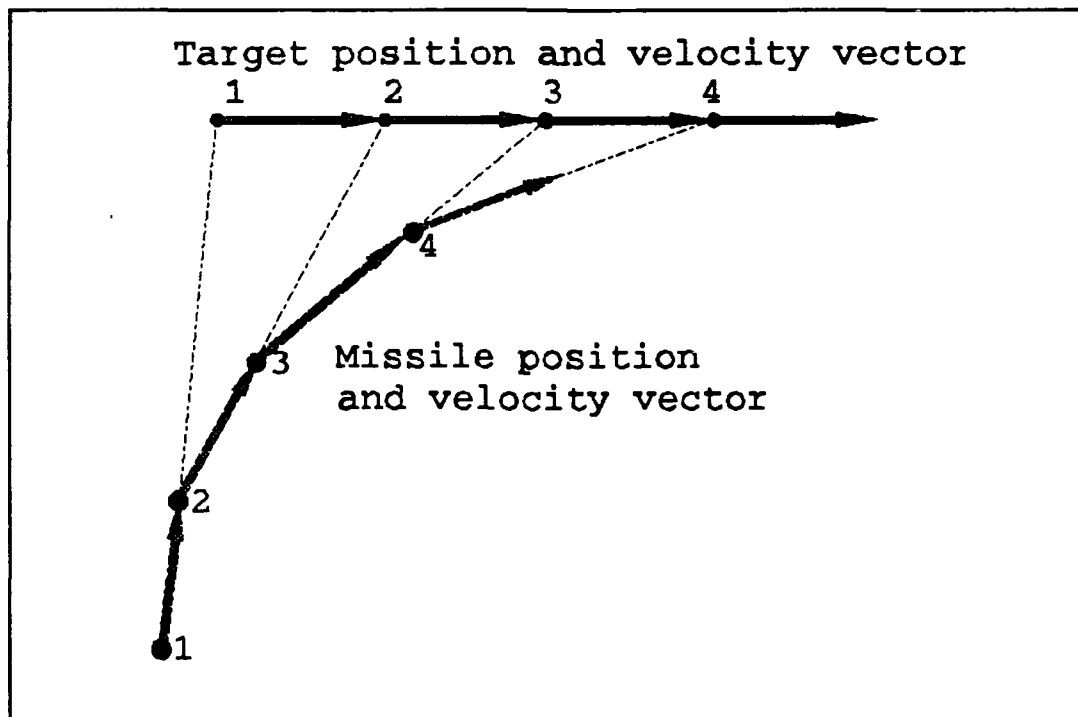


Figure 3.2 Pursuit Guidance Trajectory

2. Line-Of-Sight Guidance

The objective of a Line-of-Sight guidance system is to constrain the missile to lie as nearly as possible on the line joining the observation point and the target. This may be done by two forms which are called Command Guidance to Line-of-Sight and Beam Riding. In beam riding guidance, the target tracker maintains its radar beam on the line-of-sight and the missile tries to stay on it. In command guidance to line-of-sight, the missile receives commands to stay on the beam. In Figure 3.3, beam riding line-of-sight is illustrated [Ref. 3].

3. Proportional Navigation Guidance

In this guidance law, the missile moves in such a way that its rate of turn is proportional to the rate of turn of line-of-sight from the missile to the target. The navigation ratio is a fixed or variable ratio between the missile rate of turn and the rate of turn of the line-of-sight. This guidance system demands an acceleration command perpendicular to the line-of-sight. Since proportional navigation anticipates the future position of the target, it is effective against maneuvering targets. The proportional navigation guidance is illustrated in Figure 3.4 [Ref3].

D. CONTROL SYSTEM

The control system has two important functions; the first one is to provide a stable flight in all phases of flight and

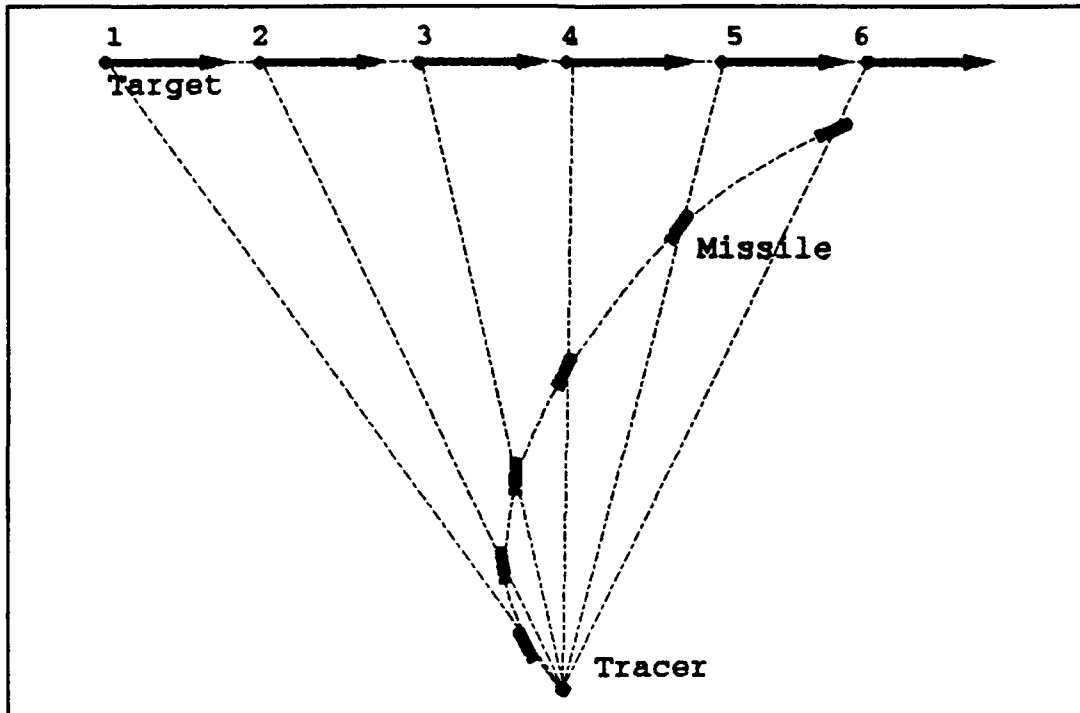


Figure 3.3 Line of Sight Guidance Trajectory

in every probable disturbance. For example, in the presence of wind, the necessary balancing commands to the control surfaces come from the control system. The second function is to follow the acceleration commands coming from the guidance system to keep the missile on an intercept course with the target.

The acceleration commands are provided by the guidance system and applied to the missile by the autopilot in the control system. In Figure 3.5a [Ref. 4] an acceleration command in j direction in missile coordinate system is seen for a missile with a velocity in i direction. The angle γ is measured from the reference axis shown in the figure. Figure 3.5b [Ref. 4] is the top view of ij plane and shows the effect of centripetal acceleration A_j in the direction of missile

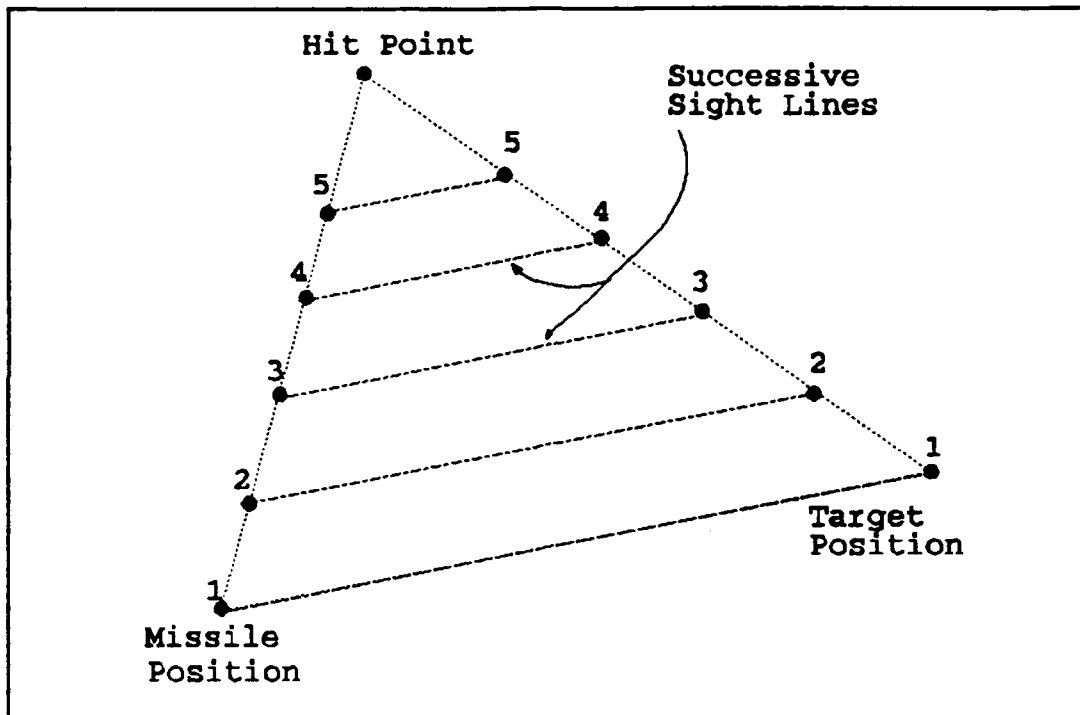


Figure 3.4 Proportional Navigation

velocity v . The change of velocity vector along j axis can be seen in Figure 3.5c. From Figure 3.5c [Ref. 4], the following equation may be written by assuming the change of direction happened in Δt seconds.

$$A_j = v \frac{\Delta \dot{\gamma}}{\Delta t} = v \dot{\gamma} \quad (3.1)$$

In Equation (3.1), commanded acceleration A_{jc} is shown in terms of tangential velocity v and angular rates $\dot{\gamma}$.

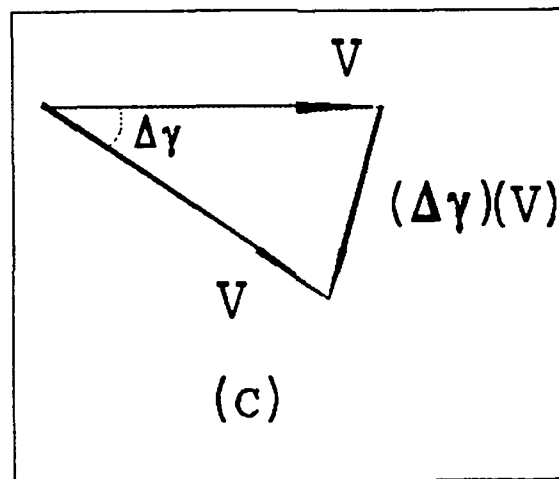
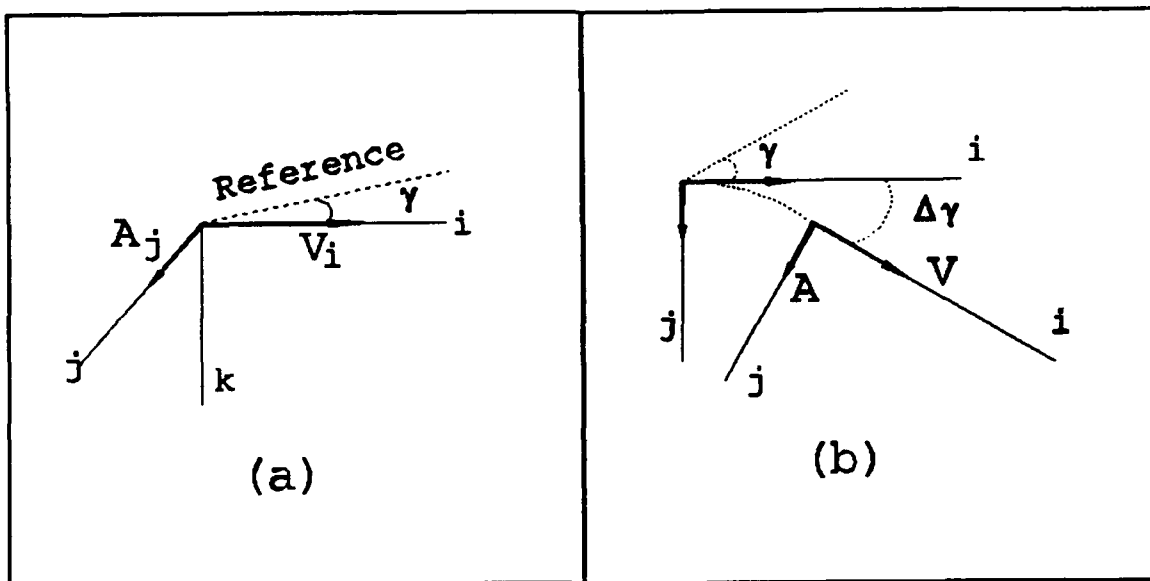


Figure 3.5 Central Acceleration Effect

IV. MISSILE MODEL AND SIMULATION

A. ASSUMPTIONS

For the missile/target engagement scenario it is necessary to have a missile model. In the simulation, the missile will be considered a point of mass. The simplified missile motion equations will be defined under the following assumptions.

- The seeker head angle rate is an estimate of the line-of-sight rate.
- The missile thrust cancels drag.
- The reference for the flight path angles is the x and y plane.

B. TWO DIMENSIONAL MISSILE TARGET GEOMETRY

Before looking to the missile model, it is advantageous to understand the equations of motion in two-dimensional geometry. In Figure 4.1, a missile and target geometry is shown in x and y directions. V_M and V_T are the velocity vectors of missile and target, respectively. γ_M and γ_T are the velocity angles from the reference line. The missile flight path angle can be expressed as

$$\gamma_M = \text{Arctan} \left(\frac{V_{MY}}{V_{MX}} \right) \quad (4.1)$$

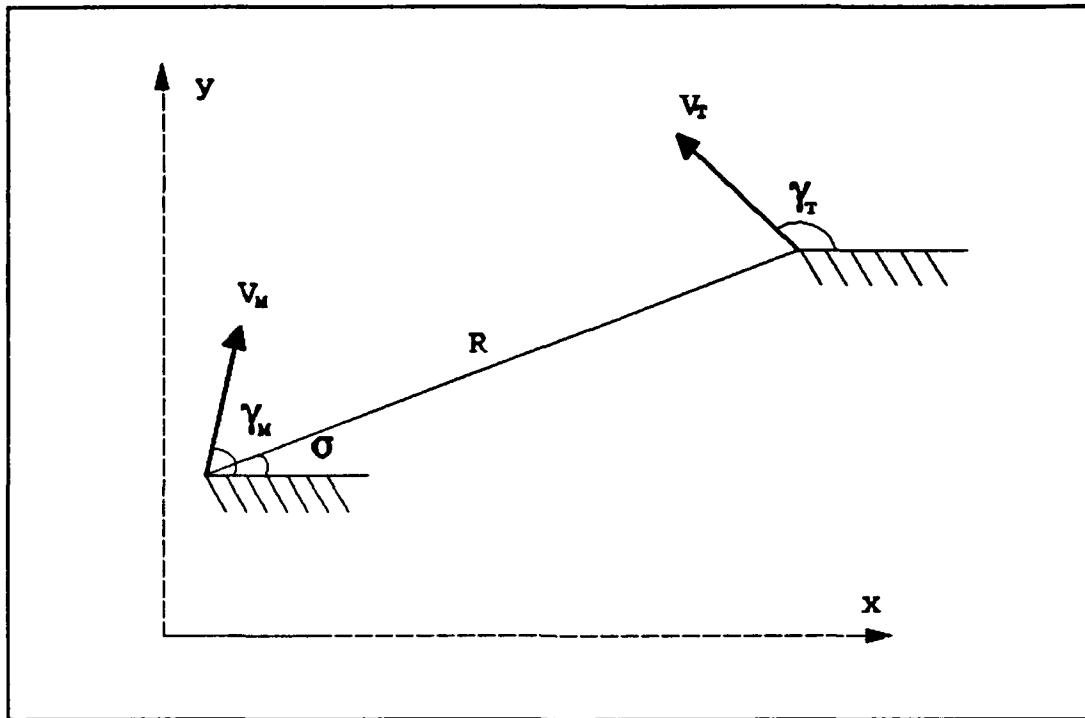


Figure 4.1 Intercept Geometry For Two Dimensions

Where V_{MX} is the velocity component in the x direction and V_{MY} is the velocity component in the y direction. From the same geometry, the target flight path can be expressed as

$$\gamma_T = \text{Arctan} \left(\frac{V_{TY}}{V_{TX}} \right) \quad (4.2)$$

Where V_{TX} and V_{TY} are the target velocity components. The range between the missile and the target is defined as

$$R = \sqrt{(x_T - x_M)^2 + (y_T - y_M)^2} \quad (4.3)$$

Where x_T , y_T , x_M , y_M are the x and y coordinates of the target and the missile.

σ is the angle of line-of-sight from the missile to the target. It is defined as

$$\sigma = \text{Arctan} \left(\frac{y_T - y_M}{x_T - x_M} \right) \quad (4.4)$$

The magnitude of velocity vectors can be defined as

$$\begin{aligned} V_M &= \sqrt{V_{Mx}^2 + V_{My}^2} \\ V_T &= \sqrt{V_{Tx}^2 + V_{Ty}^2} \end{aligned} \quad (4.5)$$

Line-of-sight rate ($\dot{\sigma}$) is a necessary factor in proportional navigation. This data is provided by the seeker head. Analytic expression for the line-of-sight rate is :

$$\dot{\sigma} = \frac{(x_T - x_M)(V_{Ty} - V_{My}) - (y_T - y_M)(V_{Tx} - V_{Mx})}{R^2} \quad (4.6)$$

C. MISSILE MODEL

1. System Signal Flow Graph

The total system signal flow graph in the x direction is illustrated in Figure 4.2 [Ref. 4]. Since proportional navigation will be simulated, the guidance system has a seeker head which provides line-of-sight rate, $(\dot{\sigma})$. The input for the autopilot is the multiplication of the navigation ratio and $\dot{\sigma}$. The output signals of the autopilot are required signals for the missile dynamics.

2. Guidance System

In signal flow graph, the guidance system includes the seeker head. A seeker head is a homing head mounted on an airborne missile. The purpose of the seeker is the tracking of the target. This is done by sensing radiation or reflected energy from the target. Tracking the target by seeker shows the angular direction to the target.

The signal flow graph of a seeker which is gimballed to the missile is shown in Figure 4.2. This seeker points at the target by rotating. Applied torques provide rotation proportional to the target offbore-sight. This can be written

$$T = I\ddot{\beta} \quad (4.7)$$

Where T is the torque, I is the moment of inertia of the seeker head and $\ddot{\beta}$ is angular acceleration. From Figure 4.2 and Equation (4.7) the resulting equation of motion is

$$\dot{\beta} = \frac{T}{I} = -K_2\beta - K_1\dot{\beta} + K_1\sigma \quad (4.8)$$

Where K_1 and K_2 determine the time constants of the seeker. The transfer function of the seeker head from input line-of-sight angle (σ) to the output seeker angle (β) can be expressed as

$$\frac{\beta(s)}{\sigma(s)} = \frac{K_1}{s^2 + K_2s + K_1} \quad (4.9)$$

The flow graph of the seeker transfer function is shown in Figure 4.2.

3. Flight Control System

Previously, it was mentioned that the control system provides a stable flight to the missile, and passes the guidance system commands to the control surfaces by keeping the missile stable. These stability requirements are satisfied by the autopilot in the control system.

The control system causes a lag in the missile system. In the present missile simulation model, the autopilot is modeled as a first order lag with a time constant, $1/\alpha$.

4. Missile Dynamics

The missile can be considered a point mass moving under the acceleration commands perpendicular to the missile velocity vector. From Figure 4.3, components of acceleration can be expressed as:

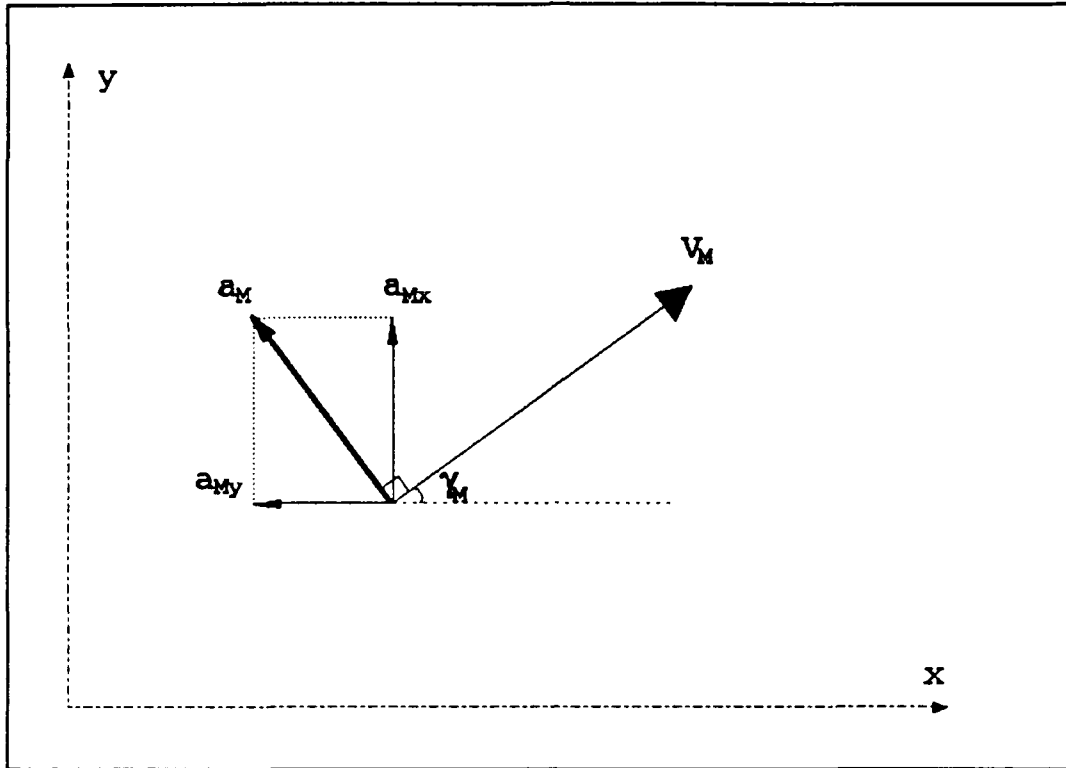


Figure 4.3 Missile Acceleration and Components

$$\begin{aligned} a_{Mx} &= -a_M \sin \gamma \\ a_{My} &= a_M \cos \gamma \end{aligned} \tag{4.10}$$

The position of the missile in the x and y plane can be found by integrating the acceleration components twice. Figure 4.4 shows the missile dynamics in two dimensions.

D. PROPORTIONAL NAVIGATION SIMULATION

In this section, the missile/target engagement will be presented in two different simulations by using proportional simulation. In the first simulation the defensive missile has

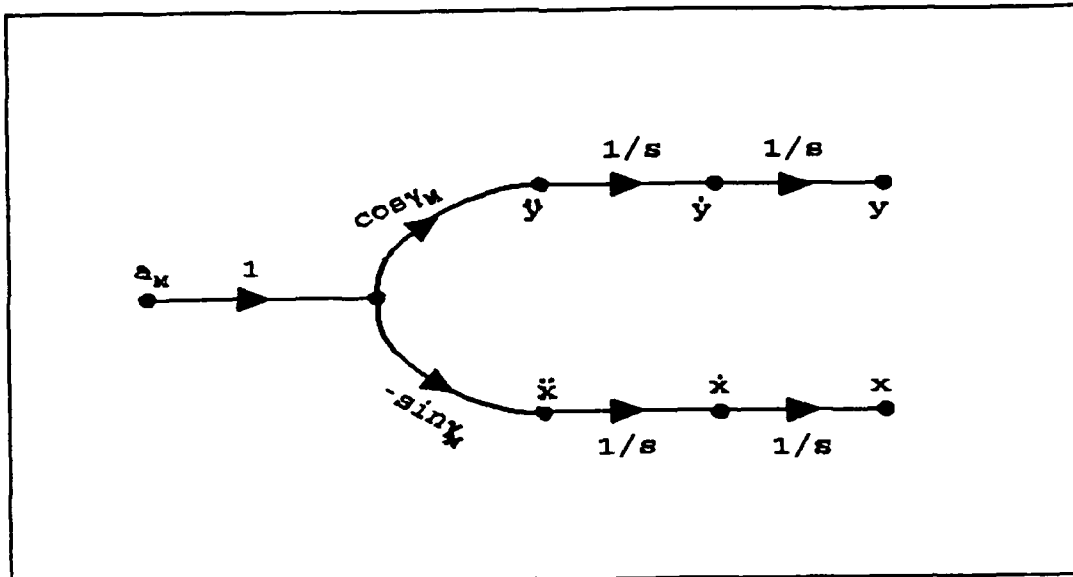


Figure 4.4 Missile Dynamics in Two Dimensions

the speed advantage; in the second simulation the target missile has the speed advantage. The following assumptions are made for both simulations

- The missile is limited to 20 g's acceleration.
- The target is on the final leg of its flight and is now on a non-maneuvering trajectory, so it has no acceleration.
- The x and y plane is the reference system for the flight paths and angles of the target and the missile.
- The miss distance will be estimated by interpolating the two most minimum ranges between the missile and the target.
- The navigation ratio is 3.25. Flight constant time constant is $1/3$ second.
- K_1 and K_2 constants in seeker head are 100 and 20, respectively.

1. Speed Advantage of Missile

In the first scenario, the defensive missile has the speed advantage over the incoming target. The initial conditions for the simulation are :

$$V_{Mx}(0) = 2000 \text{ feet/sec}$$

$$x_T(0) = 10,000 \text{ feet}$$

$$y_T(0) = 1000 \text{ feet}$$

$$V_{Tx}(0) = -1000 \text{ feet/sec}$$

All other initial conditions are zero. As shown in Figure 4.5, a successful intercept occurs and the range goes to zero. Miss distance is 0.625 feet. Figure 4.6 is a plot for the missile and the target flight paths. The target starts its motion from 10,000 feet distance and moves towards the y axis. The missile has an intercept path with the target. Figure 4.7 is a plot for the applied missile acceleration. Missile acceleration components in x and y direction are shown in Figure 4.8. At initial phase, maximum acceleration especially in y direction, is commanded. The line-of-sight angle is in Figure 4.9. Line-of-sight angle rate is shown in Figure 4.10. Initially these parameters increase, then decrease until just prior to intercept.

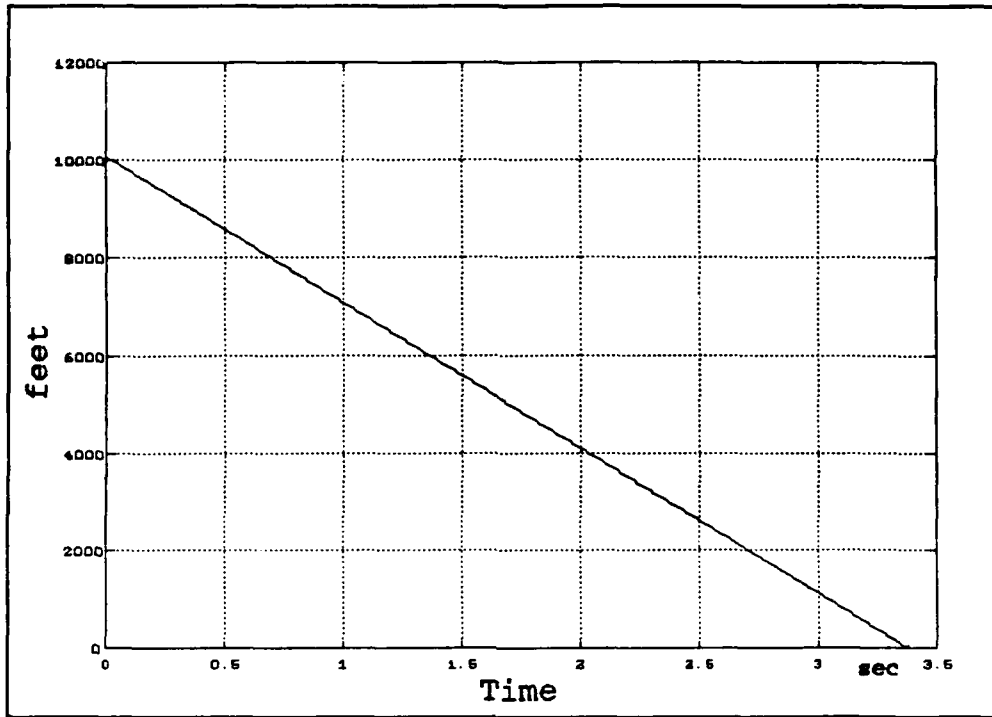


Figure 4.5 Range vs Time

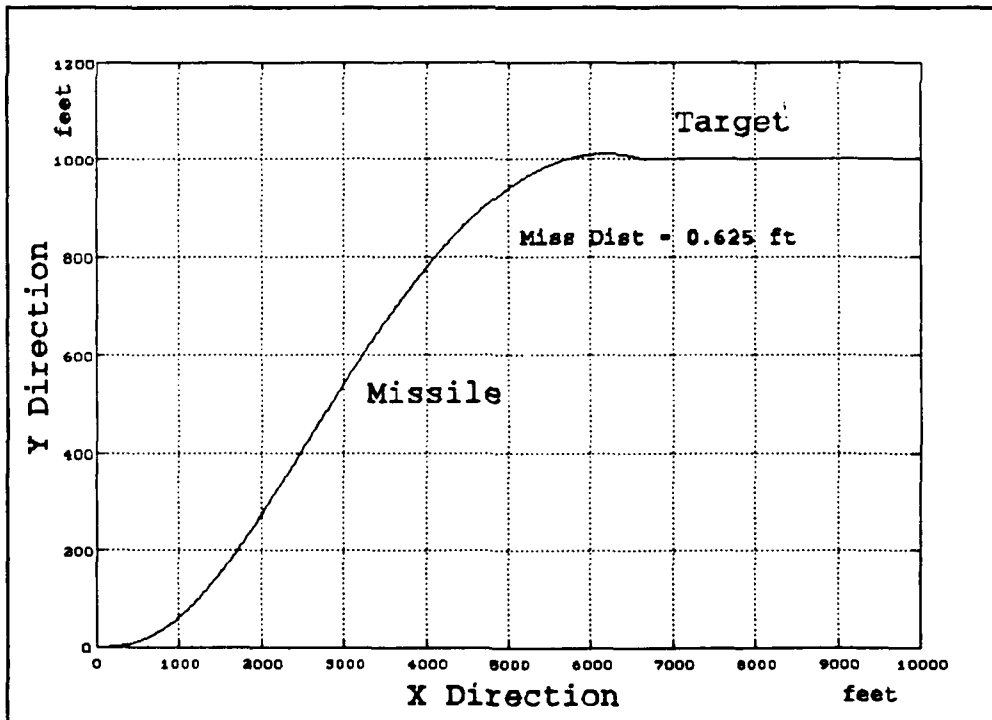


Figure 4.6 Missile and Target Flight Paths

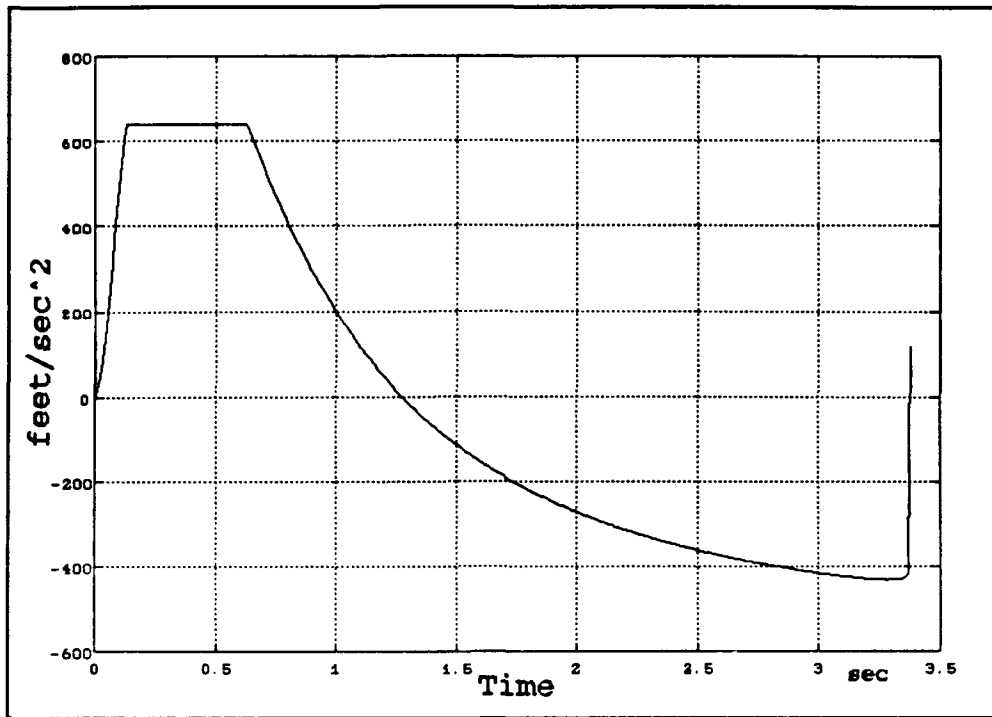


Figure 4.7 Applied Acceleration

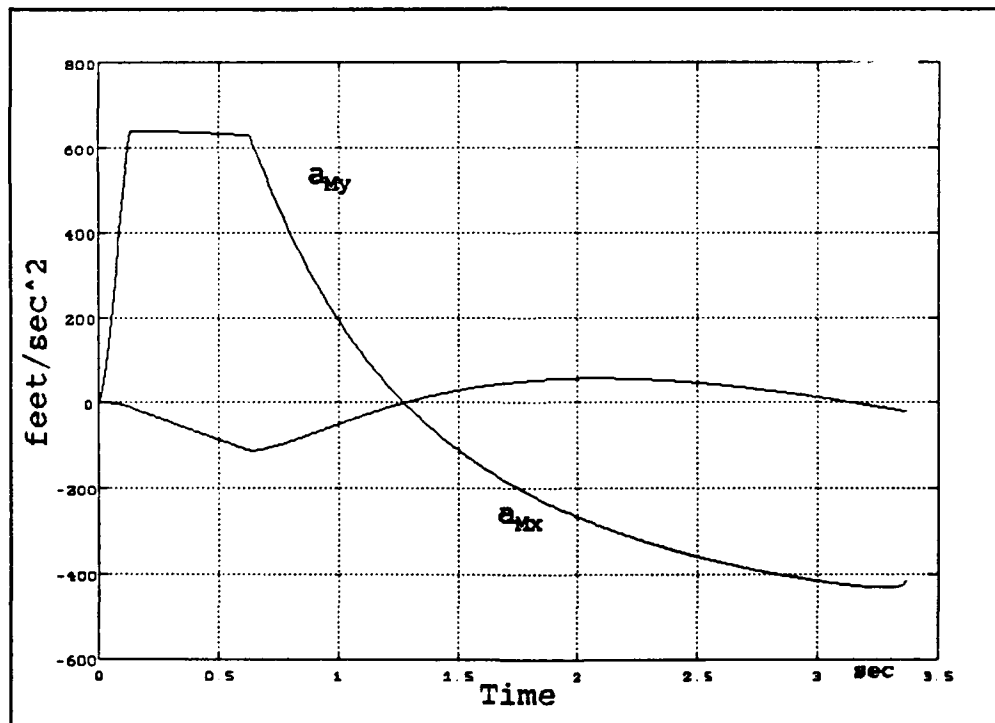


Figure 4.8 Acceleration components in x and y direction

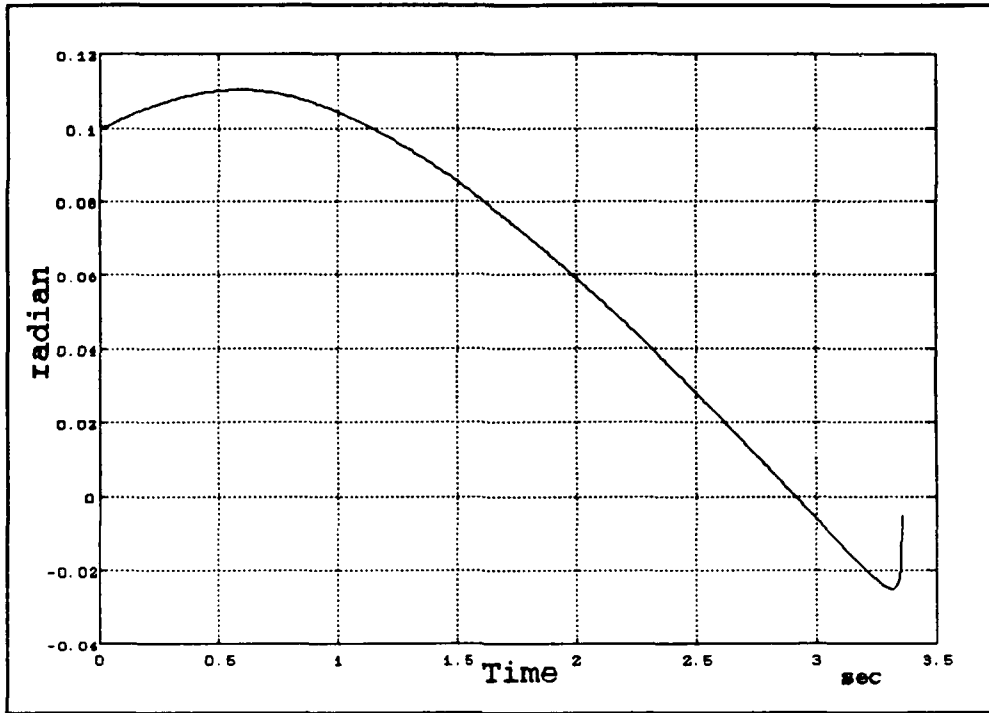


Figure 4.9 Line-of-Sight Angle

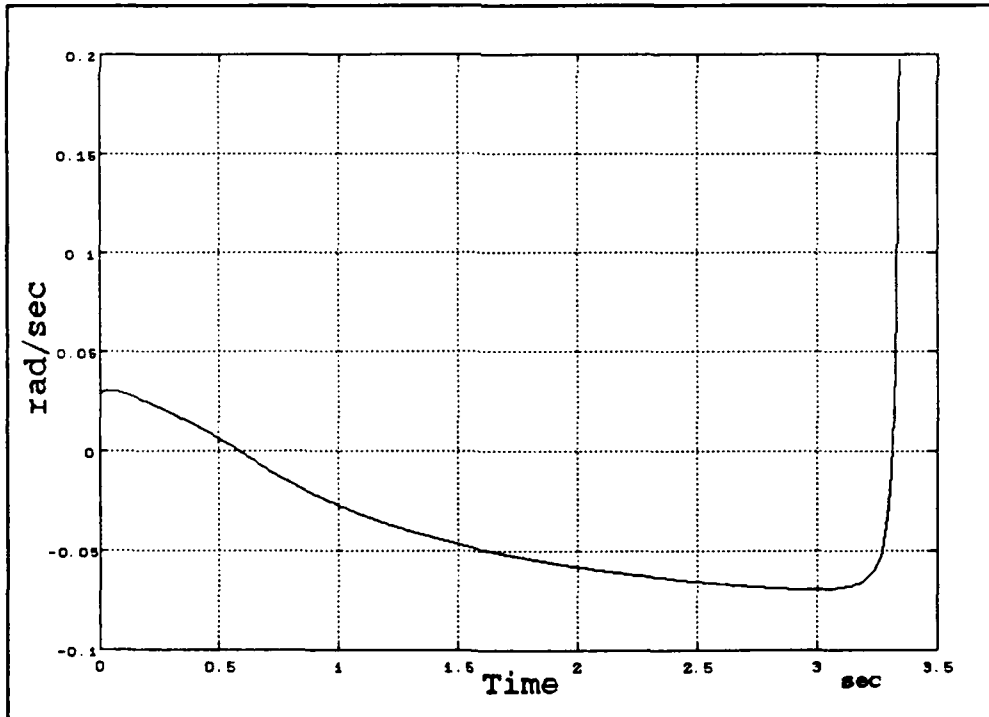


Figure 4.10 Line-of-Sight Angle Rate

2. Speed Advantage of Target

In this simulation, the incoming target has the speed advantage over the defensive missile. Only the missile and target velocities are changed from the previous simulation. The velocities are:

$$V_{Mx}(0) = 1000 \text{ feet/sec}$$

$$V_{Tx}(0) = -2000 \text{ feet/sec}$$

All other initial conditions are the same as in the previous simulation. As seen in Figure 4.11, the range goes towards zero but with an increasing miss distance. The miss distance is 17.96 feet. This is an expected result because of the speed advantage of target. Figure 4.12 shows the missile and the target flight paths. The missile still has the capability to follow the target motion. This is due to present geometry advantage for the missile and non-maneuvering target motion. Applied acceleration and acceleration components are shown in Figure 4.13 and Figure 4.14, respectively. The acceleration especially in the y direction increases during the initial phase. Figure 4.15 is a plot of the line-of-sight angle. Line-of-sight rate is shown in Figure 4.16. At initial phase line-of-sight rate increases rapidly, then decreases as the missile comes to a constant course.

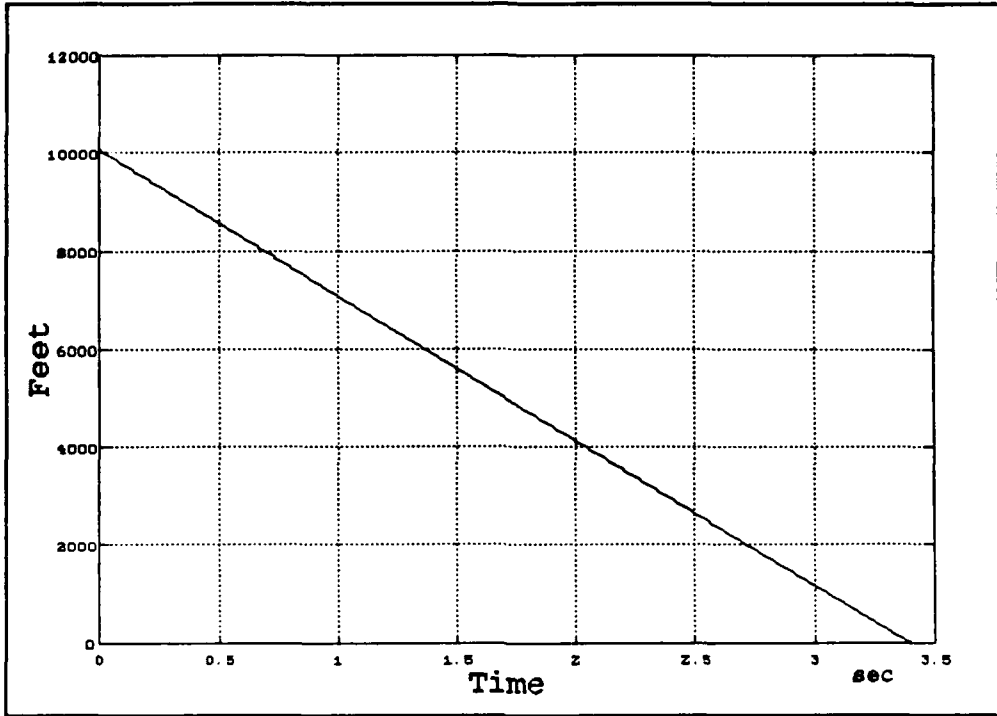


Figure 4.11 Range vs Time

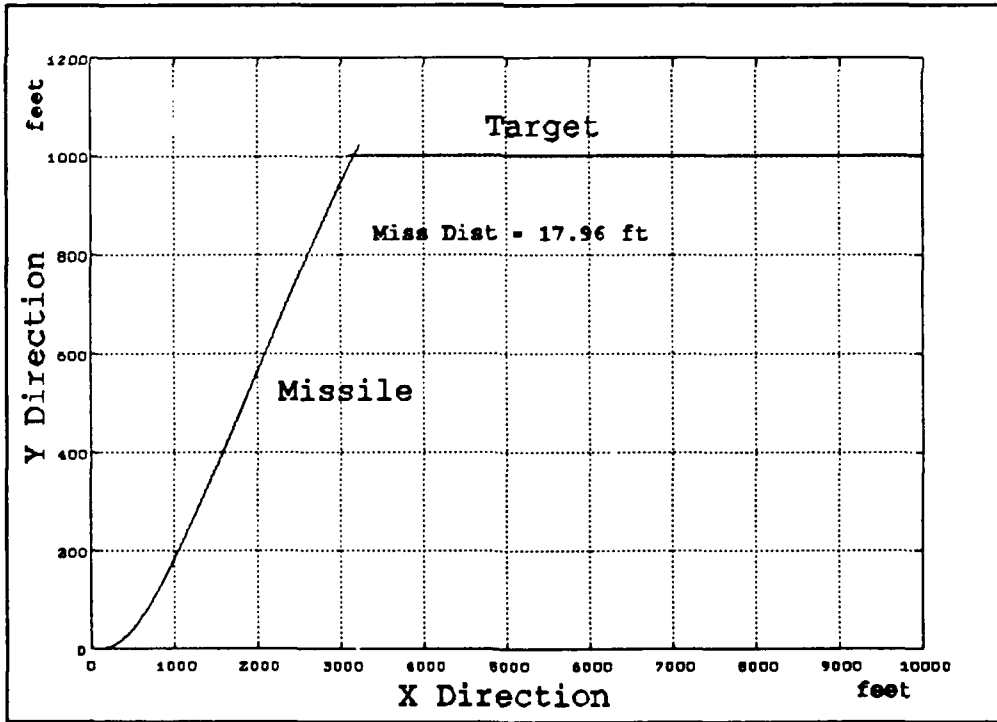


Figure 4.12 Missile and Target Trajectories

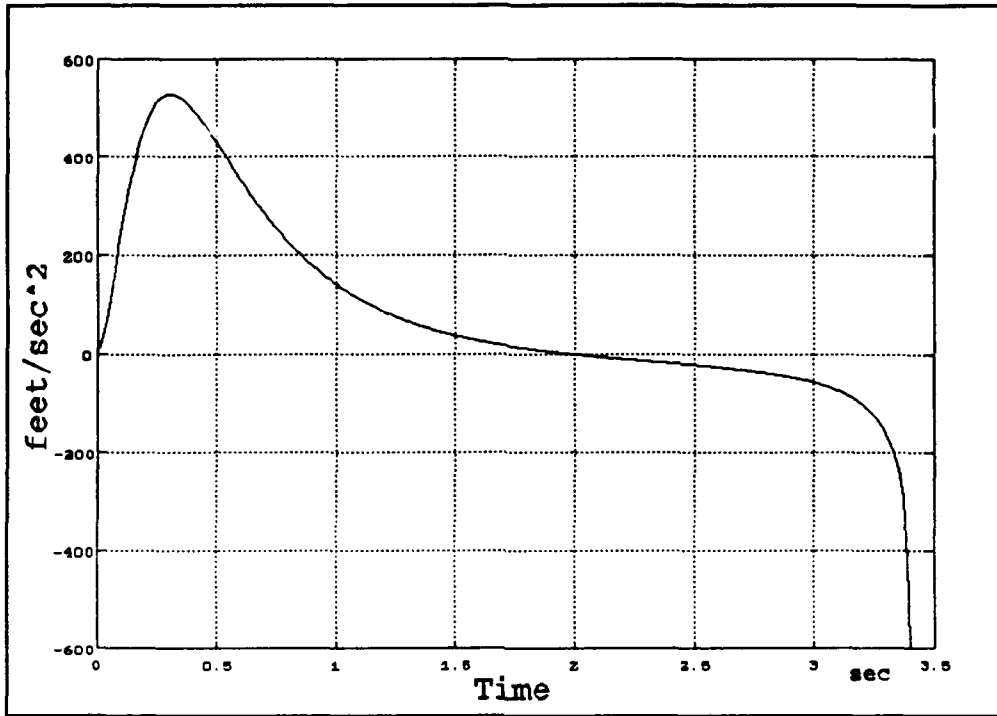


Figure 4.13 Applied Acceleration

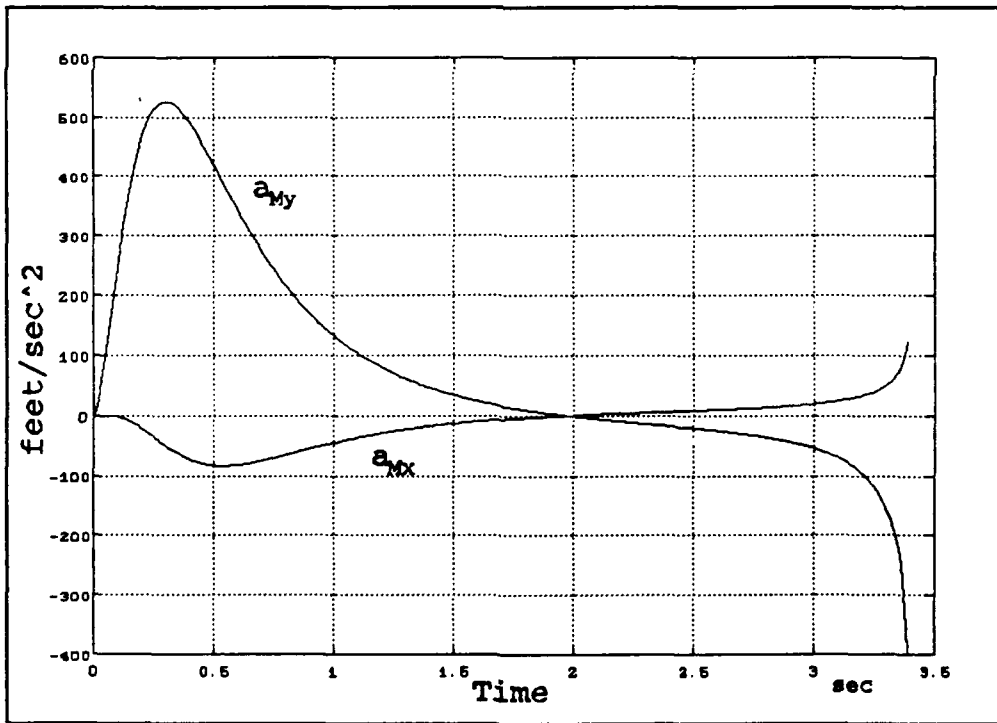


Figure 4.14 Acceleration Components

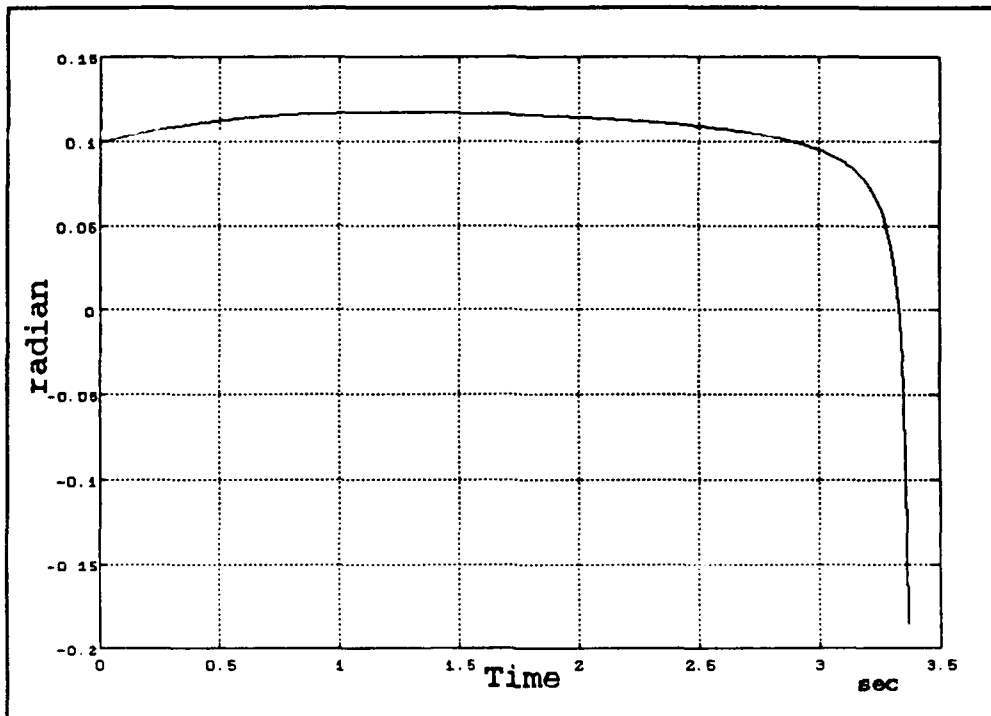


Figure 4.15 Line-of-Sight Angle

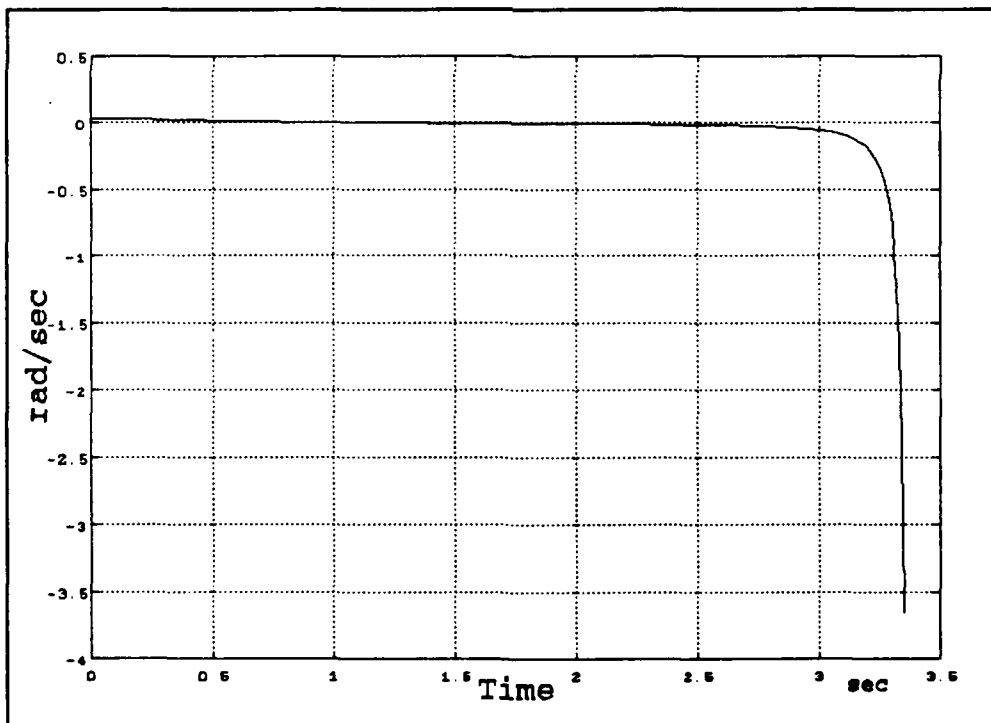


Figure 4.16 Line-of-Sight Rate

V. MISSILE APPLICATION OF THIRD ORDER CONTROLLER

A. MISSILE AND THIRD ORDER REGULATOR

When the system dynamics in Figure 4.2 are examined, the autopilot and the missile dynamics together form a third order system. This third order system is basically similar to the third order regulator switching function found in Chapter II. The difference between the two systems is the factor of $V_m \cos \gamma$ and $V_m \sin \gamma$ between $\dot{\gamma}$ and the acceleration components.

The autopilot and the missile dynamics together can be considered a third order regulator that drives the selected states to zero in minimum time as illustrated in Figure 4.1. If the right states are chosen to be driven to zero in state-space, the intercept occurs between the missile and the target.

The system signal flow graph of the missile for minimum time application is shown in Figure 5.1. In simulation, the same initial conditions used in Chapter IV for the speed advantage of the target simulation, will be used. The states which will be driven to zero are :

- The vertical distance between the missile and target and its derivative;
- The derivatives of line-of-sight angle (σ).

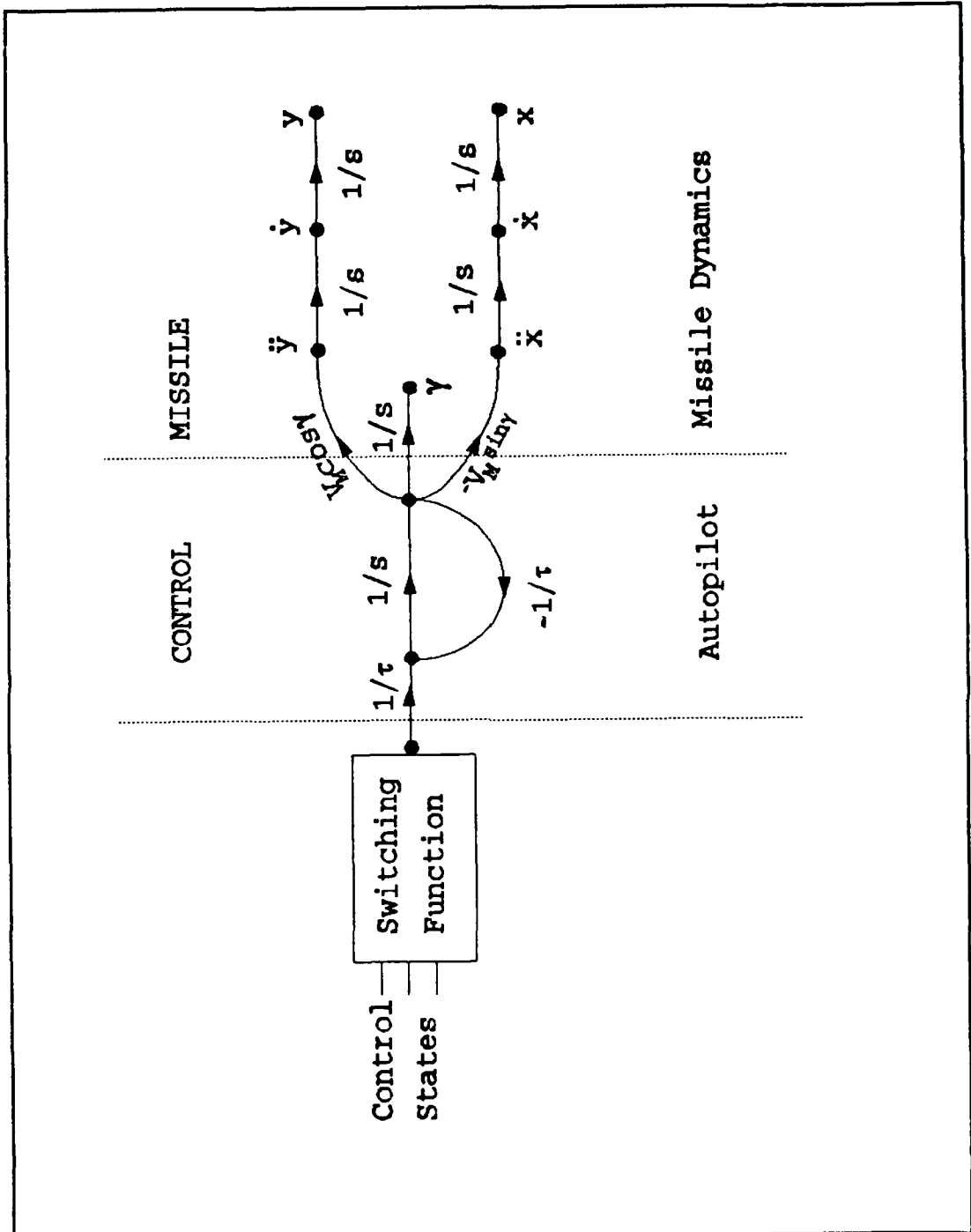


Figure 5.1 System Signal Flow Graph

B. GUIDANCE BY VERTICAL DISTANCE BETWEEN MISSILE AND TARGET

In the first approach, the states to be driven to zero are the vertical distance between the missile and the target and the first and second derivatives. The purpose is to force the missile to rise to the height of the target in minimum time, then turn on the target for head-on-collision.

Since the $V_M \cos \gamma$ is a multiplier in y channel of the flow graph, it is taken as a scaling factor for finding the uncoupled system. The y channel of the system can be considered as the following third order regulator:

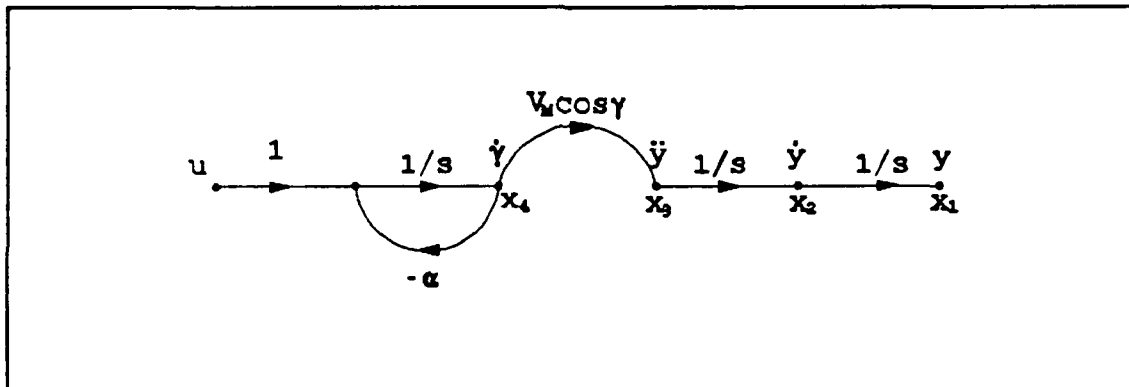


Figure 5.2 Missile y Channel as Third Order Regulator

The differential equations of the system are

$$\dot{y} = \dot{x}_1 = x_2 \quad (5.1)$$

$$\ddot{y} = \dot{x}_2 = x_3 \quad (5.2)$$

$$\begin{aligned}
\ddot{y} = \dot{x}_3 = V\dot{x}_4 &= V(-\alpha x_4 + u) \\
&= V\left(-\alpha \frac{x_3}{V} + u\right) \\
&= -\alpha x_3 + uV
\end{aligned} \tag{5.3}$$

Where $V=V_M \cos \gamma$. So the state-space of the system for y channel is

$$\begin{bmatrix} \dot{y} \\ \ddot{y} \end{bmatrix} = \begin{bmatrix} \dot{x}_1 \\ \dot{x}_2 \\ \dot{x}_3 \end{bmatrix} = \begin{bmatrix} 0 & 1 & 0 \\ 0 & 0 & 1 \\ 0 & 0 & -\alpha \end{bmatrix} \begin{bmatrix} x_1 \\ x_2 \\ x_3 \end{bmatrix} + \begin{bmatrix} 0 \\ 0 \\ V \end{bmatrix} u \tag{5.4}$$

For the uncoupled state-space, the states are defined as

$$x_1 = \frac{V/\alpha}{s^2} - \frac{V/\alpha^2}{s} + \frac{V/\alpha^2}{s+\alpha} \tag{5.5}$$

$$x_2 = \frac{V/\alpha}{s} - \frac{V/\alpha}{s+\alpha} \tag{5.6}$$

$$x_3 = \frac{V}{s+\alpha} \tag{5.7}$$

G and G⁻¹ matrices are

$$G = \begin{bmatrix} V/\alpha & -V/\alpha^2 & V/\alpha^2 \\ 0 & V/\alpha & -V/\alpha \\ 0 & 0 & V \end{bmatrix} \quad \text{and} \quad G^{-1} = \begin{bmatrix} \alpha/V & 1/V & 0 \\ 0 & \alpha/V & 1/V \\ 0 & 0 & 1/V \end{bmatrix} \tag{5.8}$$

The uncoupled state-space is

$$\begin{bmatrix} \dot{y}_1 \\ \dot{y}_2 \\ \dot{y}_3 \end{bmatrix} = \begin{bmatrix} 0 & 1 & 0 \\ 0 & 0 & 0 \\ 0 & 0 & -\alpha \end{bmatrix} \begin{bmatrix} y_1 \\ y_2 \\ y_3 \end{bmatrix} + \begin{bmatrix} 0 \\ 1 \\ 1 \end{bmatrix} u \quad (5.9)$$

It is seen that the uncoupled system is the same for the third order regulator example in Chapter II. Thus, the switching law is the same as in Equation (2.35) for the uncoupled state-space. But the transformation from uncoupled state-space to normal state-space by Equation (2.36) will be different. The uncoupled states in terms of normal states are

$$\begin{aligned} y_1 &= \frac{\alpha}{V} x_1 + \frac{1}{V} x_2 \\ y_2 &= \frac{\alpha}{V} x_2 + \frac{1}{V} x_3 \\ y_3 &= \frac{1}{V} x_3 = \dot{y} \end{aligned} \quad (5.10)$$

It is seen that all states are divided by $V_M \cos \gamma$. Therefore, the switching law from Equation (2.38) is obtained by dividing the states by $V_M \cos \gamma$.

After running the simulation, the missile rises to the height of the target and then turns onto the target for head-on-collision. The flight paths of the missile and the target are in Figure 5.3. The range according to time is shown in

Figure 5.4. The miss distance is 0.07 feet. The vertical distance between the missile and the target according to time is shown in Figure 5.5. It is seen that the vertical distance is driven to zero and kept at that value until intercept occurs. The acceleration and the acceleration components are shown in Figures 5.6 and 5.7, respectively. Acceleration, especially at the beginning of flight, is applied at its maximum. Acceleration in y direction starts with a high value and decreases as the vertical distance decreases.

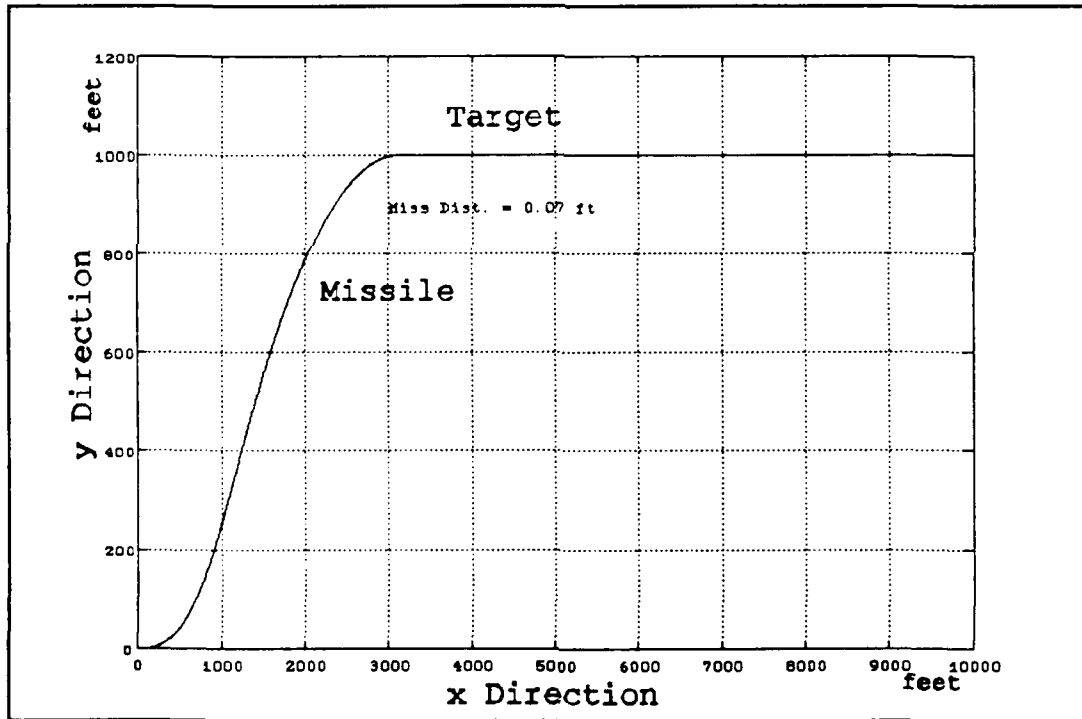


Figure 5.3 Missile and Target Trajectories

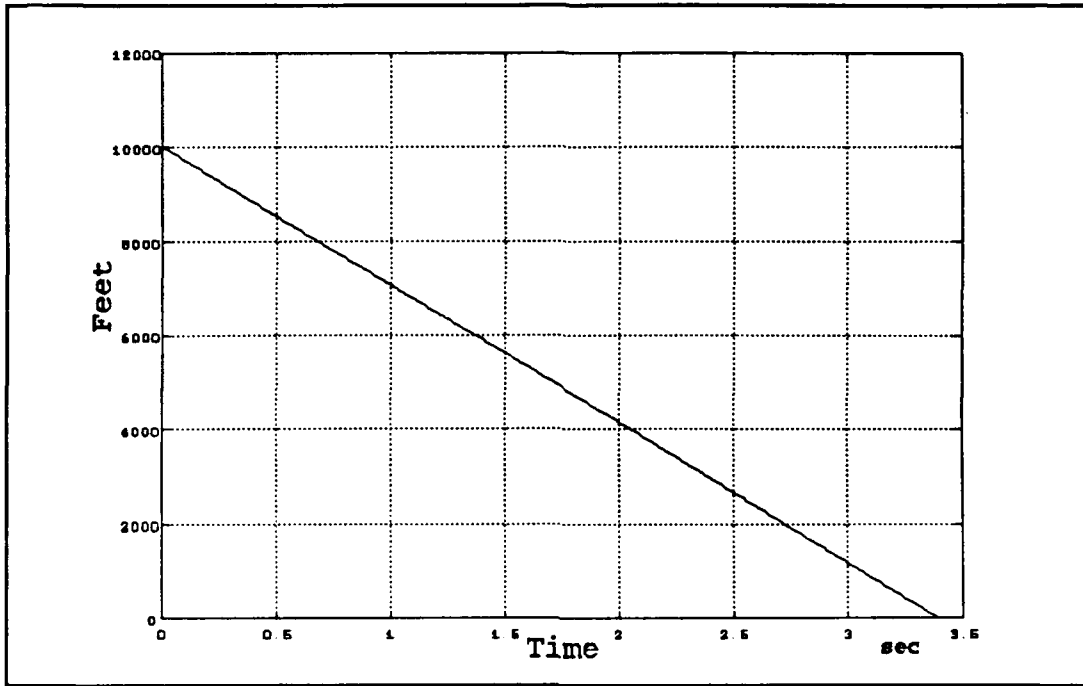


Figure 5.4 Range vs Time

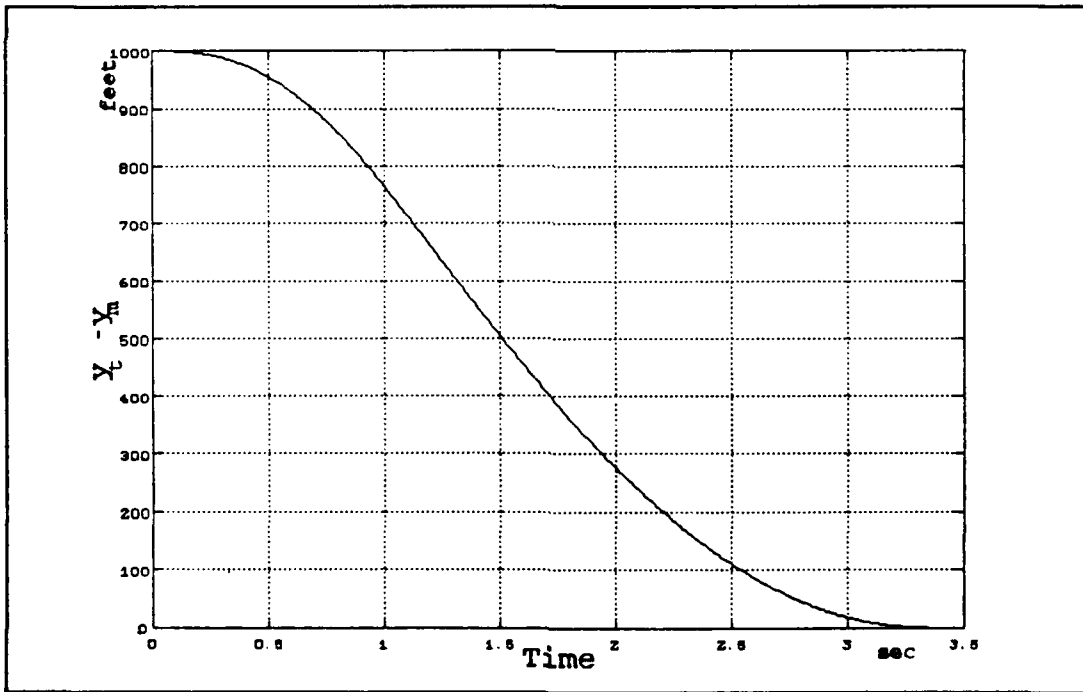


Figure 5.5 Vertical Distance vs Time

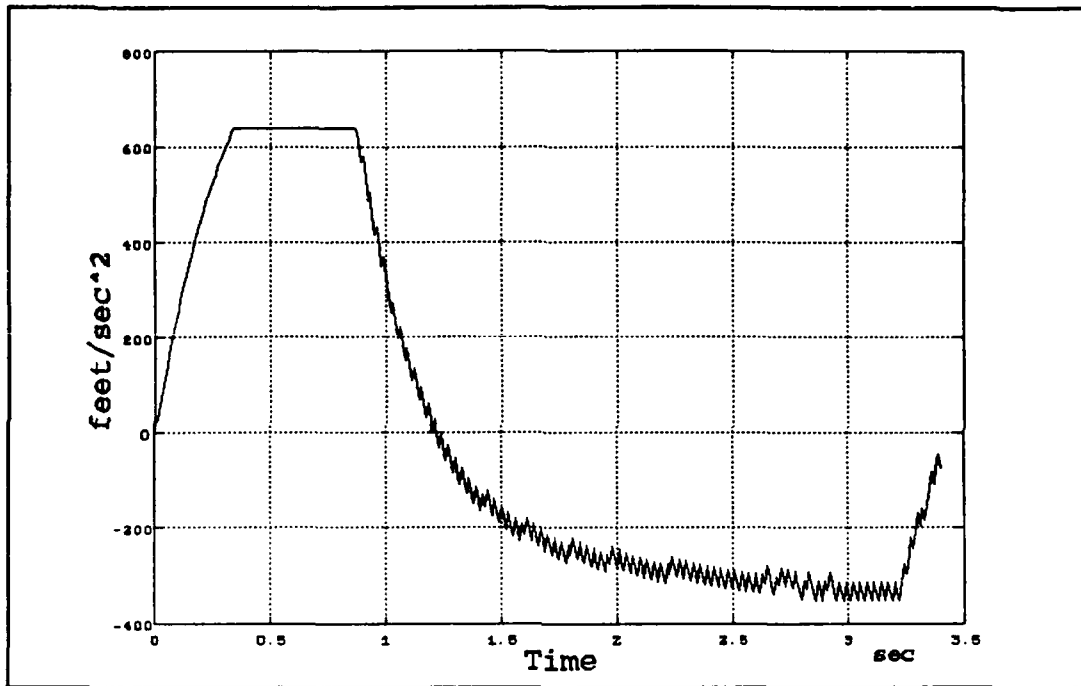


Figure 5.6 Applied Acceleration

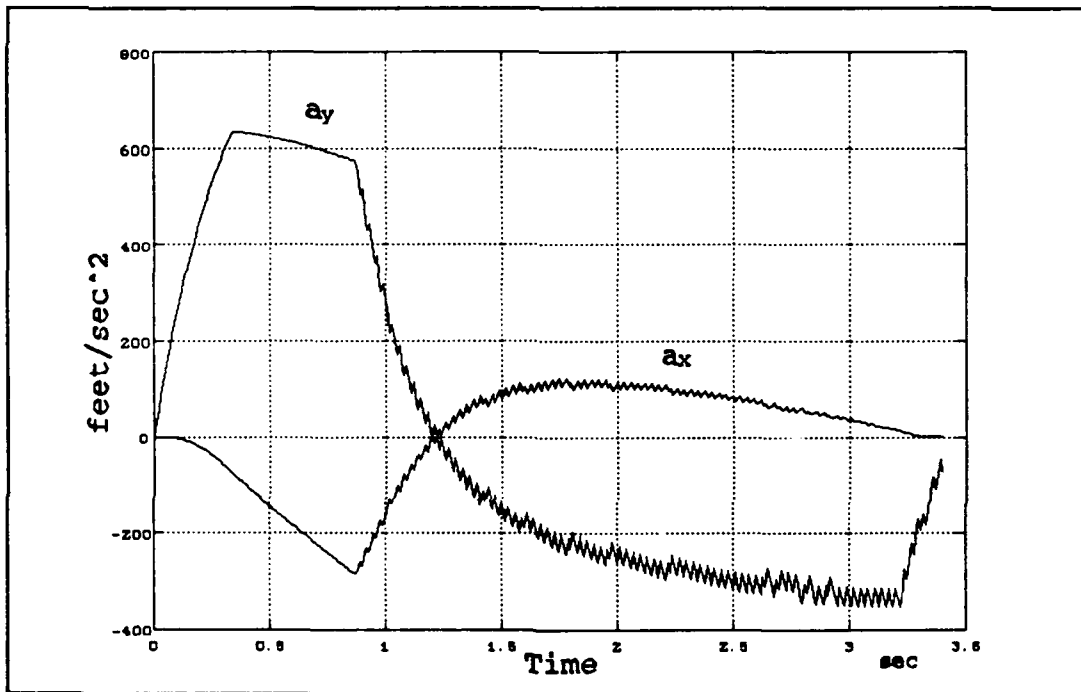


Figure 5.7 Acceleration Components

C. GUIDANCE BY DERIVATIVES OF σ

The second group of states which is chosen are the derivatives of line-of-sight angle $(\dot{\sigma}, \ddot{\sigma}, \dddot{\sigma})$. If the $\dot{\sigma}$ is driven to zero, the σ becomes constant. If the relative velocity is decreasing and the line-of-sight is constant, intercept occurs between the missile and target. This is the theory of Proportional Navigation Guidance and illustrated in Figure 3.4.

We can have the σ and its derivatives analytically from Figure 4.1. In an actual application, these values can be estimated by a Kalman filter or a Luenberger observer. Line-of-sight angle is given by Equation (4.4). Derivatives of σ are

$$\dot{\sigma} = \frac{xV_y - yV_x}{R^2} \quad (5.11)$$

$$\ddot{\sigma} = \frac{xa_y - ya_x}{R^2} - \frac{2(xV_x + yV_y)(xV_y - yV_x)}{R^4} \quad (5.12)$$

$$\begin{aligned} \dddot{\sigma} = & \frac{(V_x a_y + x\ddot{y} - V_y a_x - y\ddot{x})(R^2) - 2(xV_x + yV_y)(xa_y - ya_x)}{R^4} \\ & - \frac{2(V_x^2 + xa_x + V_y^2 + ya_y)(xV_y - yV_x) + 2(xa_y - ya_x)(xV_x + yV_y)}{R^4} \quad (5.13) \\ & + \frac{8(xV_x + yV_y)^2(xV_y - yV_x)}{R^6} \end{aligned}$$

Where

$$x = x_T - x_M$$

$$y = y_T - y_M$$

$$V_x = V_{Tx} - V_{Mx}$$

$$V_y = V_{Ty} - V_{My}$$

$$a_x = a_{Tx} - a_{Mx}$$

$$a_y = a_{Ty} - a_{My}$$

After the simulation, we found that the control drives the derivatives of σ to zero and intercept occurs. Flight paths of the missile and the target are shown in Figure 5.9. The range is plotted in Figure 5.10. Miss distance is 0.045 feet. The line-of-sight angle is shown in Figure 5.11. Figure 5.12 shows the line-of-sight angle rate. It is seen that the control drives the line-of-sight angle rate to zero, so the line-of-sight is kept constant and intercept occurs. Acceleration and its components are shown in Figures 5.13 and 5.14.

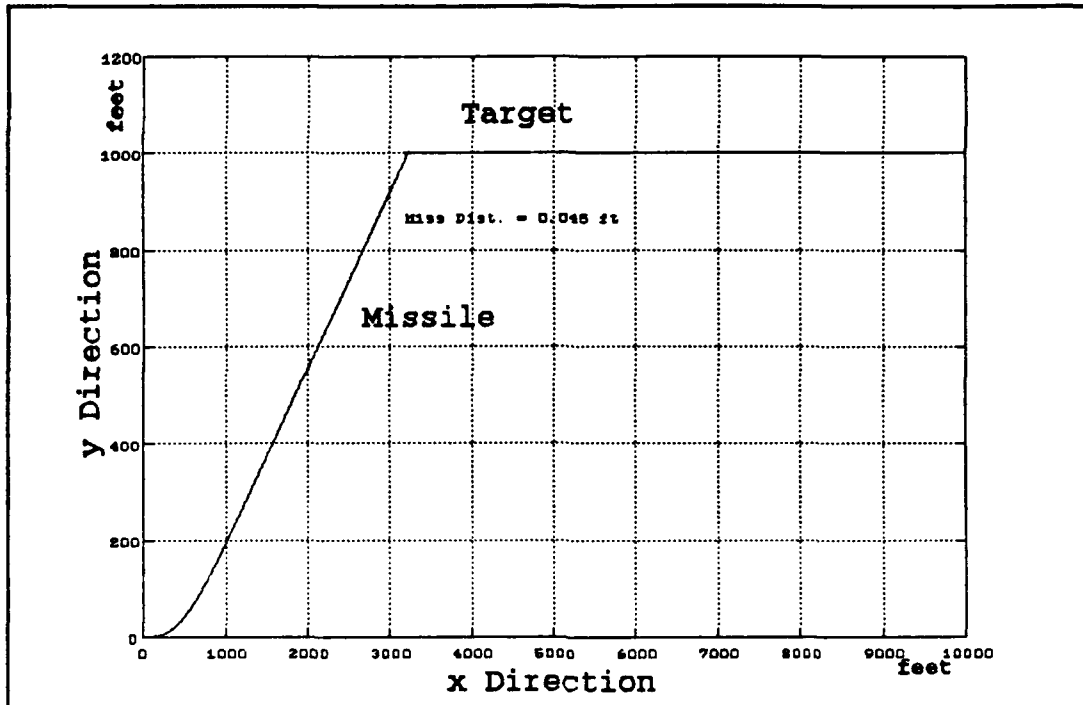


Figure 5.8 Missile and Target Flight Paths

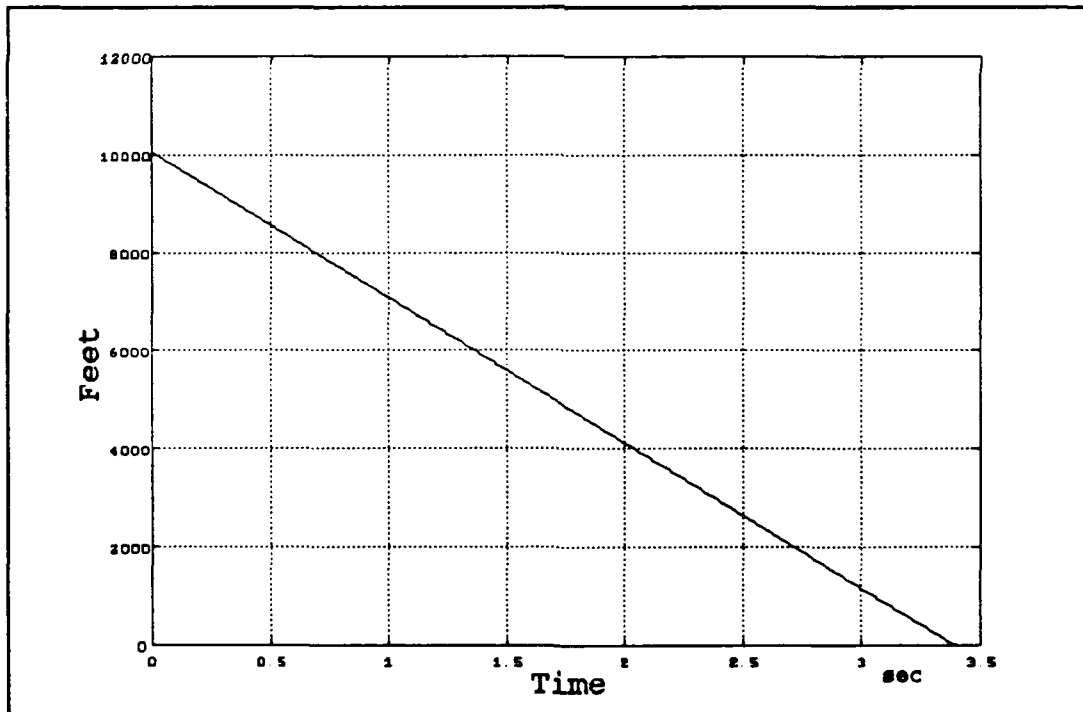


Figure 5.9 Range vs Time

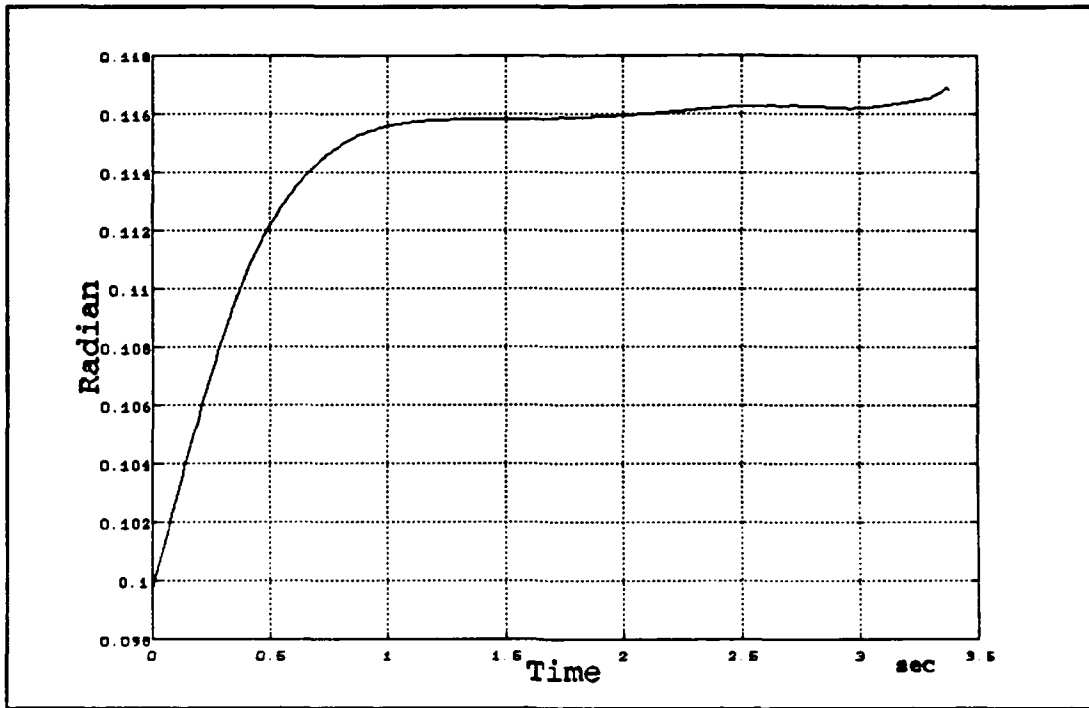


Figure 5.10 Line-Of-Sight Angle vs Time

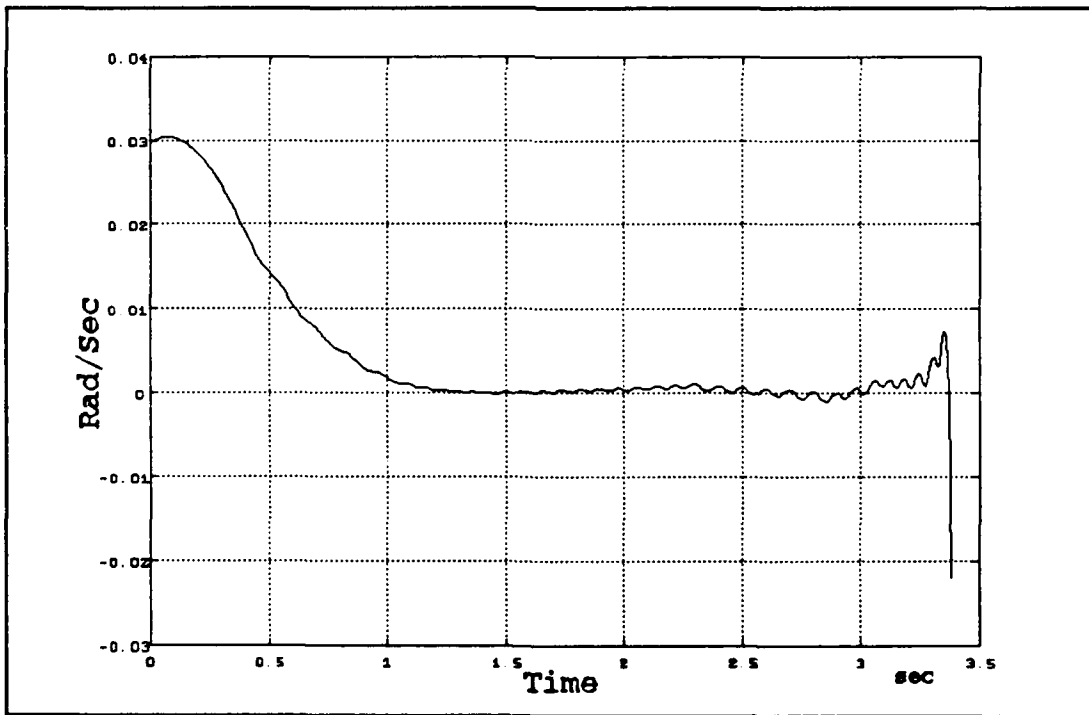


Figure 5.11 Line-Of-Sight Angle Rate

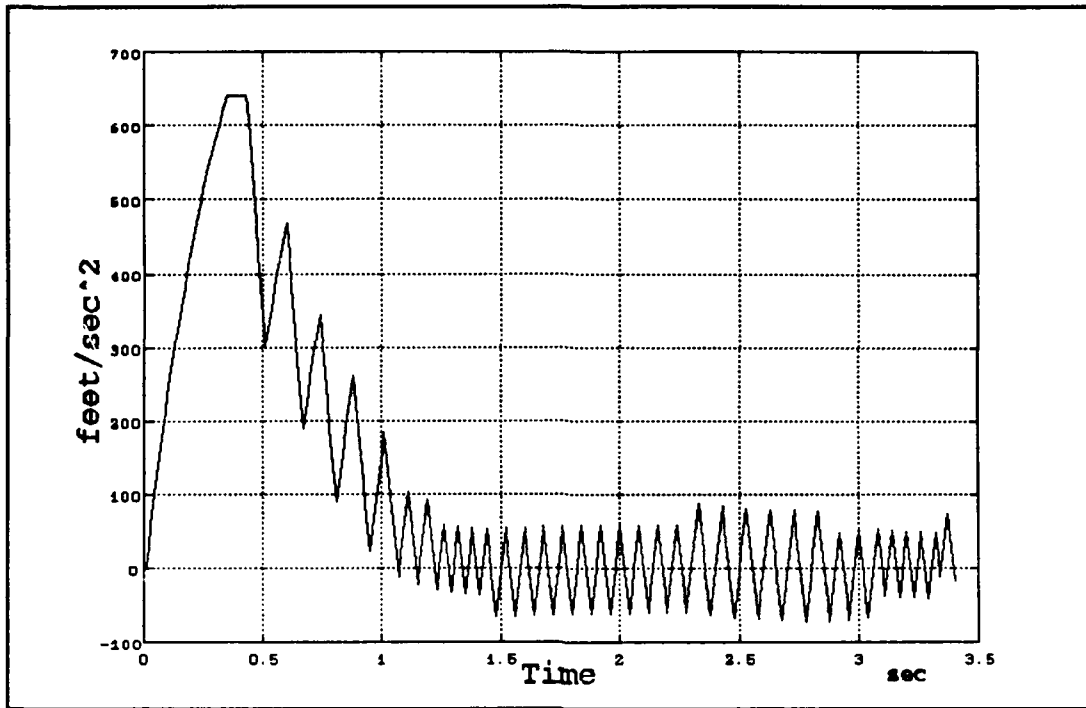


Figure 5.12 Applied Acceleration

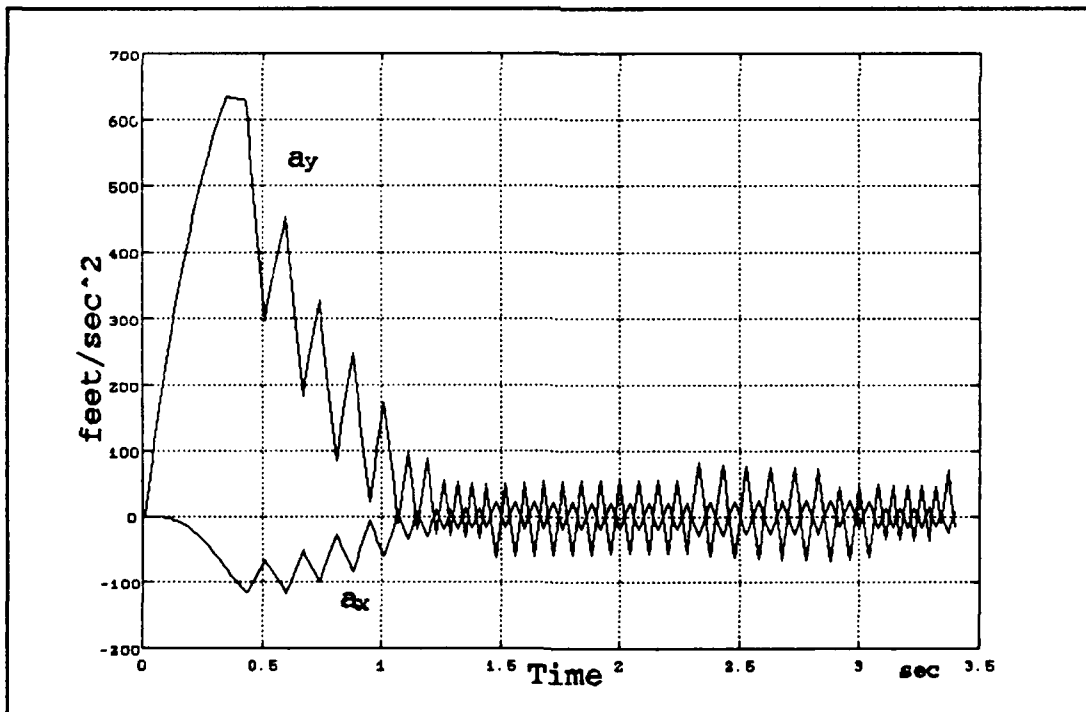


Figure 5.13 Acceleration Components

VI. CONCLUSIONS

A third order minimum time switching law was developed. The switching law that was found, was applied to the third order fast reaction missile defense problem. The Proportional Navigation Guidance is applied to the same problem for comparison.

Minimum time application was established using two different approaches. One was with the vertical distance and derivatives, the other was the first, second and third order derivatives of Line-of-Sight angle. Both approaches gave more effective results than Proportional Navigation Guidance.

Since *bang bang* control always uses negative or positive maximum control effort, another control logic is necessary to shut off the control effort when the desired conditions are met. Otherwise, the system starts a chattering mode or limit cycles. This may be a subject for future projects.

APPENDIX

1. PROPNAV.M

```
% Missile/Target engagement simulation
% Proportional Guidance
% Target has a non-maneuvering flight
% Program terminates when the range starts to increase
% Miss Distance is found by interpolating the minimum range

clear;clg
Nr=3.25; % Navigation Ratio
alp=3; % 1/alpha = Autopilot time constant
maxac=640; % Allowed maximum acceleration
Am=[0 1 0 0; % Missile state matrices
    0 0 0 0;
    0 0 0 1;
    0 0 0 0];
Bm=[0 0;1 0;0 0;0 1];
Aa=[-alp]; % Autopilot states
Ba=[alp];
As=[ 0 1; % Seeker states
    -100 -20];
Bs=[ 0;100];

% DISCRETIZE THE SYSTEM
dt=0.01; % Sampling time
[phim,delm]=c2d(Am,Bm,dt); % Missile system
[phit]=[phim];[delt]=[delm]; % Target system
[phia,dela]=c2d(Aa,Ba,dt); % Autopilot
[phis,dels]=c2d(As,Bs,dt); % Seeker head
% INITIALIZE THE STATES
xm(:,1)=[ 0 % xm0 [x;xd;y;yd]
          1000 % xdm0
           0 % ym0
           0]; % ydm0

xt(:,1)=[10000 % xt0 [x;xd;y;yd]
         -2000 % xdt0
           1000 % yt0
           0]; % ydt0
```

```

R(1)=sqrt((xt(1,1)-xm(1,1))^2+(xt(3,1)-xm(3,1))^2);
time(1)=0; % Time
am(1)=0;amx(1)=0;amy(1)=0; % Acceleration
gamadmis(1)=0; % Missile flight angle
beta(:,1)=[0;0]; % Seeker head angle
% BEGIN SIMULATION LOOP
Tf=15; % Simulation time
kmax=Tf/dt+1;
for i=1:kmax-1
    v_mis(i)=sqrt(xm(2,i)^2+xm(4,i)^2); % Missile velocity
    gama_mis(i)=atan2(xm(4,i),xm(2,i)); % Missile vel. angle
    sigma(1,i)=atan2((xt(3,i)-xm(3,i)),(xt(1,i)-xm(1,i)));
    beta(:,i+1)=phis*beta(:,i)+dels*sigma(i);
% Input For the Autopilot=betadot*Nr
    gamadmis(i+1)=phia*gamadmis(i)+dela*Nr*beta(2,i+1);
% Missile Acceleration
    am(i+1)=v_mis(i)*gamadmis(i+1);
    if abs(am(i+1)) > maxac % Check for max. acceleration
        am(i+1)=maxac*sign(am(i+1));
    end
% Acceleration is perpendicular to gama
    u(:,i+1)=[-sin(gama_mis(i))*am(i+1);
              cos(gama_mis(i))*am(i+1)];
% Update missile & target states
    xm(:,i+1)=phim*xm(:,i)+delm*u(:,i+1);
    xt(:,i+1)=phit*xt(:,i)+delm*[0;0];

R(i+1)=sqrt((xt(1,i+1)-xm(1,i+1))^2+(xt(3,i+1)-xm(3,i+1))^2);
time(i+1)=time(i)+dt;

% Check for the min. distance
    if abs(R(i+1)) > abs(R(i))
xms=[xm(3,i-1:i+1);xm(4,i-1:i+1);xm(1,i-1:i+1);xm(2,i-1:i+1)];
xts=[xt(3,i-1:i+1);xt(4,i-1:i+1);xt(1,i-1:i+1);xt(2,i-1:i+1)];
        r1 = interp(xms(:,1:2),xts(:,1:2)); % [Ref. 5]
        r2 = interp(xms(:,2:3),xts(:,2:3));
        rmin=min([r1 r2]);
        break % Terminate if distance is min.
    end
end
end

```

```

% PLOT RESULTS

% Flight paths of missile and target
plot(xt(1,1:i+1),xt(3,1:i+1),xm(1,1:i+1),xm(3,1:i+1))
title('Flight Paths');
gtext(['rmin = ',num2str(rmin)]);pause

% Acceleration Components
plot(time(1:i),u(1,1:i),time(1:i),u(2,1:i));
title('Acceleration Components');pause;

% Missile acceleration
plot(time(1:i+1),am(1:i+1));
title('Missile Acceleration');pause;

% Line-of-sight rate
plot(time(1:i),beta(2,1:i));
title('Line-of-Sight Rate');pause

% Line-of-Sight angle
plot(time(1:i),sigma(1:i));
title('Line of sight');pause

% Range
plot(time(1:i+1),R(1:i+1))
title('Range')

```

2. YYDYDD.M

```
% Missile/Target engagement simulation
% Control by Third Order Minimum Time Controller
% Control States: Vertical Distance and derivatives
% Missile acceleration limited to 640 ft/sec2
% Program terminates when the range starts increasing
% Miss Distance is found by interpolating minimum distance
```

```
clear; clg
alp=3; % 1/alp = Autopilot time constant
N=1;
maxac=640;
Am=[0 1 0 0; % Missile matrices
    0 0 0 0;
    0 0 0 1;
    0 0 0 0];
Bm=[0 0; 1 0; 0 0; 0 1];
Aa=[0 1; % Autopilot states
    0 -alp];
Ba=[0; alp];
% DISCRETIZE THE SYSTEM
dt=0.01; % Sampling time
[phim, delm]=c2d(Am, Bm, dt);
[phit]=[phim];
[delt]=[delm];
[phia, dela]=c2d(Aa, Ba, dt);
% INITIALIZE STATES
xm(:, 1:2)=[ 0 10; % xm0
            1000 1000; % xdm0
            0 0; % ym0
            0 0]; % ydm0

xt(:, 1:2)=[ 10000 9980; % xt0
            -2000 -2000; % xdt0
            1000 1000; % yt0
            0 0]; % ydt0

R(1)=sqrt((xt(1,1)-xm(1,1))^2+(xt(3,1)-xm(3,1))^2);
R(2)=sqrt((xt(1,2)-xm(1,2))^2+(xt(3,2)-xm(3,2))^2);
time(1:2)=[0 0];
```

```

gmis(1)=0;
gamamis(:,1:2)=[0 0;0 0];
amy(1:2)=[0 0];
v_mis(1)=1000;aax(1)=0;aay(1)=0;
% SWITCHING LAW
ax=0; ay=0;
Vx=(xt(2,1)-xm(2,1)); Vy=xt(4,1)-xm(4,1);
x=(xt(1,1)-xm(1,1)); y=xt(3,1)-xm(3,1);
xs1(1)=y; xs2(1)=Vy; xs3(1)=0;
u(1)=N*swth_law(xs1,xs2,xs3,alp,N);
%BEGIN SIMULATION LOOP
Tf=15;
kmax=Tf/dt+1;
for i=2:kmax-1
    % Missile velocity
    v_mis(i)=sqrt(xm(2,i)^2+xm(4,i)^2);
    gmis(i)=atan2(xm(4,i),xm(2,i));
    xs1(i)=(xt(3,i)-xm(3,i))/(v_mis(i)*cos(gmis(i)));
    xs2(i)=(xt(4,i)-xm(4,i))/(v_mis(i)*cos(gmis(i)));
    xs3(i)=-gamamis(2,i);%-amy(i);%
    u(i)=N*swth_law(xs1(i),xs2(i),xs3(i),alp,N);
    % Input for the autopilot = u
    gamamis(:,i+1)=phia*gamamis(:,i)+dela*u(i);
    % Missile acceleration
    am(i+1)=v_mis(i)*gamamis(2,i+1);
    if abs(am(i+1)) > maxac
        am(i+1)=maxac*sign(am(i+1));
    end

    % Acceleration components
    amx(i+1)=-am(i+1)*sin(gmis(i));
    amy(i+1)= am(i+1)*cos(gmis(i));

    % Update missile and target states
    xm(:,i+1)=phim*xm(:,i)+delm*[ amx(i+1); amy(i+1)];
    xt(:,i+1)=phit*xt(:,i)+delm*[0;0];

R(i+1)=sqrt((xt(1,i+1)-xm(1,i+1))^2+(xt(3,i+1)-xm(3,i+1))^2);

time(i+1)=time(i)+dt;
if (abs(R(i+1)) > abs(R(i)))

```

```

xms=[xm(3,i-1:i+1);xm(4,i-1:i+1);xm(1,i-1:i+1);xm(2,i-1:i+1)];

xts=[xt(3,i-1:i+1);xt(4,i-1:i+1);xt(1,i-1:i+1);xt(2,i-1:i+1)];
    r1 = interp(xms(:,1:2),xts(:,1:2));      % [Ref. 5]
    r2 = interp(xms(:,2:3),xts(:,2:3));
    rmin=min([r1 r2]);
    break
end
end

% PLOT RESULTS
% Flight paths
plot(xm(1,1:3:i+1),xm(3,1:3:i+1),xt(1,1:3:i+1),xt(3,1:3:i+1))
title('Flightpaths');
gtext(['rmin=',num2str(rmin)]);pause;

% Control input
axis([0 time(i)+0.1 -N-N/10 N+N/10])
plot(time(1:2:i),u(1:2:i),time(1:2:i),u(1:2:i),'*');
title('U');pause;axis;

% Missile acceleration
axis([0 time(i)+0.1 -maxac-maxac/25 maxac+maxac/25])
plot(time(1:2:i+1),am(1:2:i+1));
title('Missile acceleration');pause;axis;

% Missile velocity angle
plot(time(1:2:i),gmis(1,1:2:i));
title('Gama');
pause;

% Missile velocity
plot(time(1:2:i),v_mis(1:2:i),time(1:2:i),v_mis(1:2:i),'*');
title('Missile velocity');pause;

% y states
plot(time(1:2:i),xt(3,1:2:i)-xm(3,1:2:i));
title('(Y_target - Y_missile vs Time ');
pause;

```

3. SIGMDER.M

```
% Missile/Target engagement simulation
% Control by Third Order Minimum Time Controller
% Control States: Derivatives of Sigma
% Missile acceleration limited to 640 ft/sec2
% Program terminates when the range starts increasing
% Miss Distance is found by interpolating minimum distance
clear;clc
alp=3;
N=1;
maxac=640;
Am=[0 1 0 0;                % Missile matrices
    0 0 0 0;
    0 0 0 1;
    0 0 0 0];
Bm=[0 0;
    1 0;
    0 0;
    0 1];
Aa=[0 1;                    % Autopilot states
    0 -alp];
Ba=[0;alp];
dt=0.01;
Tf=25;
kmax=Tf/dt+1;
% INITIALIZE STATES
xm(:,1)=[ 0;                % xm0
          1000;             % xdm0
          0;                % ym0
          0];              % ydm0
xt(:,1)=[ 10000;           % xt0
          -2000;           % xdt0
          1000;            % yt0
          0];              % ydt0
xm(:,2)=[ 10;              % xm0
          1000;            % xdm0
          0;                % ym0
          0];              % ydm0
xt(:,2)=[ 9980;           % xt0
          -2000;           % xdt0
```

```

        1000;      % yt0
        0];      % ydt0
R(1)=sqrt((xt(1,1)-xm(1,1))^2+(xt(3,1)-xm(3,1))^2);
R(2)=sqrt((xt(1,2)-xm(1,2))^2+(xt(3,2)-xm(3,2))^2);
gamamis(:,1:2)=[0 0;0 0];
am(1:2)=[0 0];amx(1:2)=[0 0]; amy(1:2)=[0 0];
time(1:2)=[0 dt];
[phim,delm]=c2d(Am,Bm,dt);
[phit]=[phim];
[delt]=[delm];
[phia,dela]=c2d(Aa,Ba,dt);
v_mis(1)=1000;aax(1)=0;aay(1)=0;
ax=0;          ay=0;
Vx=(xt(2,1)-xm(2,1)); Vy=xt(4,1)-xm(4,1);
x=(xt(1,1)-xm(1,1)); y=xt(3,1)-xm(3,1);
sigma(1,1)=atan2(y,x);
sigma(2,1)=(Vy*x-Vx*y)/(x^2+y^2);
sigma(3,1)=(ay*x-ax*y)/R(1)^2-2*(x*Vx+y*Vy)*(x*Vy-y*Vx)/R(1)^4;
sigma(3,1)=(ay*x-ax*y)/(x^2+y^2)-2*(x*Vx+y*Vy)*(x*Vy-y*Vx)/(x^2+y^2)^2;
xs1(1)=sigma(2,1);xs2(1)=sigma(3,1);xs3(1)=0;
u(1)=N*swth_law(xs1,xs2,xs3,alp,N);
for i=2:kmax-1
    % Missile velocity
    v_mis(i)=sqrt(xm(2,i)^2+xm(4,i)^2);
    gama_mis(i)=atan2(xm(4,i),xm(2,i));
    ay=-amy(i); ax=-amx(i);
    Vy=xt(4,i)-xm(4,i); Vx=(xt(2,i)-xm(2,i));
    y=xt(3,i)-xm(3,i); x=(xt(1,i)-xm(1,i));
    aay(i)=(-amy(i-1)+v_mis(i-1)*cos(gamamis(1,i))*u(i-1));
    aax(i)=(-amx(i-1)+v_mis(i-1)*sin(gamamis(1,i))*u(i-1));
    sigma(1,i)=atan2(y,x);
    sigma(2,i)=(Vy*x-Vx*y)/(x^2+y^2);

sigma(3,i)=(ay*x-ax*y)/(x^2+y^2)-2*(x*Vx+y*Vy)*(x*Vy-y*Vx)/(x^2+y^2)^2;
    xs1(i)=sigma(2,i);xs2(i)=sigma(3,i);
    xs3(i)=(Vx*ay+x*aay(i)-Vy*ax-y*aax(i))/R(i)^2-...
        2*(x*Vx+y*Vy)*(x*ay-y*ax)/R(i)^4-...
    2*((Vx^2+x*aax+Vy^2+y*ay)*(x*Vy-y*Vx)+(x*ay-y*ax)*(x*Vx+y*Vy))/R(i)^4+...

```

```

8*(x*Vx+y*Vy)^2*(x*Vy-y*Vx)/R(i)^6;
u(i)=N*swth_law(xs1(i),xs2(i),xs3(i),alp,N);
% END SWITCHING LAW
% Input for the autopilot = u
gamamis(:,i+1)=phia*gamamis(:,i)+dela*u(i);
% Missile acceleration
am(i+1)=v_mis(i)*gamamis(2,i+1);
if abs(am(i+1)) > maxac
    am(i+1)=maxac*sign(am(i+1));
end
% Acceleration components
amx(i+1)=-am(i+1)*sin(gamamis(1,i+1));
amy(i+1)= am(i+1)*cos(gamamis(1,i+1));
% Update missile and target states
xm(:,i+1)=phim*xm(:,i)+delm*[ amx(i+1); amy(i+1)];
xt(:,i+1)=phit*xt(:,i)+delm*[0;0];

R(i+1)=sqrt((xt(1,i+1)-xm(1,i+1))^2+(xt(3,i+1)-xm(3,i+1))^2);
time(i+1)=time(i)+dt;
if (abs(R(i+1)) > abs(R(i)))

xms=[xm(3,i-1:i+1);xm(4,i-1:i+1);xm(1,i-1:i+1);xm(2,i-1:i+1)];

xts=[xt(3,i-1:i+1);xt(4,i-1:i+1);xt(1,i-1:i+1);xt(2,i-1:i+1)];
r1 = interp(xms(:,1:2),xts(:,1:2)); % [Ref. 5]
r2 = interp(xms(:,2:3),xts(:,2:3));
rmin=min([r1 r2]);
break
end
end
% PLOT RESULTS
% Flight paths
plot(xt(1,1:3:i+1),xt(3,1:3:i+1),'*',xm(1,1:3:i+1),xm(3,1:3:
i+1))
title('Flight paths');
gtext(['rmin=',num2str(rmin)]);
pause;
% Control input
plot(time(1:2:i),u(1:2:i),time(1:2:i),u(1:2:i),'*');
title('U');
pause;

```

```

% Missile acceleration

plot(time(1:2:i+1),am(1:2:i+1),time(1:2:i+1),am(1:2:i+1),'*');
title('Missile acceleration');
pause;
% Missile velocity angle
plot(time(1:2:i),gamamis(1,1:2:i),time(1:2:i),gama_mis(1,1:2:i),'*');
title('Gama');xlabel('Time');ylabel('Radian')
pause;
% Missile velocity
plot(time(1:2:i),v_mis(1:2:i),time(1:2:i),v_mis(1:2:i),'*');
title('Missile velocity');
;pause
% y states
plot(time(1:2:i),xt(3,1:2:i)-xm(3,1:2:i));
title('(Y_target - Y_missile) vs Time');pause;%meta sigcd6
% range
    plot(time,R);title('range');pause;%meta range
% sigma
plot(time(1:i),sigma(1,1:i));title('sigma');
pause;
% sigmadot
    plot(time(1:i),sigma(2,1:i));title('sigmadot');pause
    %meta sigmadot
    plot(time,amx,time,amy);title('comp. ');pause;%meta comp

```

4. SWTH_LAW.M

% Function calculates the sign of the control

```
function[s]=swth_law(x1,x2,x3,alp,N);  
w=sign((alp*x1+x2)+((alp*x2+x3)*abs(alp*x2+x3)/(2*N)));  
f=(alp*x1+x2)+w*((alp*x2+x3)^2/(2*N));  
z=sqrt(abs(f)/N);  
s=sign(w*((N*exp(alp*z)/alp)-(2*N/alp))+((exp(-alp*z)*...  
exp(-w*alp*(alp*x2+x3)/N))*(x3+w*N/alp)));
```

REFERENCES

- [1] Kirk, D.E., *Optimal Control Theory, An Introduction*, p.1 and pp. 240-259, Prentice-Hall, 1970
- [2] Lee, R.G. and others, *Guided Weapons*, Brassey's Defense Publishers, 1983
- [3] Garnell, P., *Guided Weapon Systems*, Pergamon Press, 1980
- [4] Titus, H.A., *Missile Guidance*, Naval Postgraduate School, 1990 (unpublished notes for EC4340)
- [5] Colin, C.R., *Second and Third Order Minimum Time Controllers and Missile Adjoints*, p. 78, MSEE Thesis in Naval Postgraduate School, 1991

INITIAL DISTRIBUTION LIST

1. Defense Technical Information Center 2
Cameron Station
Alexandra, Virginia 22304-6145
2. Library Code 52 2
Naval Postgraduate School
Monterey, California 93943-5002
3. Chairman, Code EC 1
Department of Electrical and Computer Engineering
Naval Postgraduate School
Monterey, California 93943
4. Prof. Harold A. Titus, Code EC/TS 2
Department of Electrical and Computer Engineering
Naval Postgraduate School
Monterey, California 93943
5. Prof. Jeffrey B. Burl, Code EC/BL 1
Department of Electrical and Computer Engineering
Naval Postgraduate School
Monterey, California 93943
6. Deniz Kuvvetleri Komutanlığı 1
Personel Başkanlığı
Bakanlıklar ANKARA TURKEY
7. Deniz Harp Okulu Komutanlığı 1
Okul Kütüphanesi
Tuzla İSTANBUL TURKEY
8. Hakan Karazeybek 2
Camii Kebir Mah.
41. Sokak No: 4
Seferihisar İZMİR TURKEY
9. Kayhan Vardareri 1
Ege Mah. Kıvrak Sokak
No: 16/3
BALIKESİR TURKEY